
DETECTING SEMANTIC BACKDOORS IN A MYSTERY SHOPPING SCENARIO

Árpád Berta¹, Gábor Danner¹, István Hegedűs¹, and Márk Jelasity^{1,2}

¹Institute of Informatics, University of Szeged, Szeged, Hungary

²HUN-REN—SZTE Research Group on AI, Szeged, Hungary

October 20, 2025

{berta, danner, ihegedus, jelasity}@inf.u-szeged.hu

ABSTRACT

Detecting semantic backdoors in classification models—where some classes can be activated by certain natural, but out-of-distribution inputs—is an important problem that has received relatively little attention. Semantic backdoors are significantly harder to detect than backdoors that are based on trigger patterns due to the lack of such clearly identifiable patterns. We tackle this problem under the assumption that the clean training dataset and the training recipe of the model are both known. These assumptions are motivated by a consumer protection scenario, in which the responsible authority performs mystery shopping to test a machine learning service provider. In this scenario, the authority uses the provider’s resources and tools to train a model on a given dataset and tests whether the provider included a backdoor. In our proposed approach, the authority creates a reference model pool by training a small number of clean and poisoned models using trusted infrastructure, and calibrates a model distance threshold to identify clean models. We propose and experimentally analyze a number of approaches to compute model distances and we also test a scenario where the provider performs an adaptive attack to avoid detection. The most reliable method is based on requesting adversarial training from the provider. The model distance is best measured using a set of input samples generated by inverting the models in such a way as to maximize the distance from clean samples. With these settings, our method can often completely separate clean and poisoned models, and it proves to be superior to state-of-the-art backdoor detectors as well. Source code available at <https://github.com/szegedai/SemanticBackdoorDetection>.

Keywords semantic backdoor detection, adversarial training, mystery shopping, consumer protection

1 Introduction

Artificial intelligence (AI) safety is a key concern in today’s quickly changing AI landscape. Apart from a very significant research effort into safety problems such as adversarial robustness [1], model backdoors [2], and alignment [3], to name a few, governments and corporations have both started to create regulation, organizations, and tools to enhance safety.

AI-related regulations and guidelines require enforcement as well to be effective. To enforce measures for AI safety, the authorities need a rich set of tools to verify AI systems. The wide variety of backdoor detectors are an important part of such a toolset (see Section 2). Here, we focus on extending this toolset with a semantic backdoor detector. This is necessary, because semantic backdoors cannot be reliably detected by generic backdoor detectors, they need a dedicated approach. This is because, in this case, the attacker poisons a model by adding out-of-distribution (OOD) samples to the training set to secretly extend the possible behaviors of the system in a completely arbitrary manner [4]. There is no

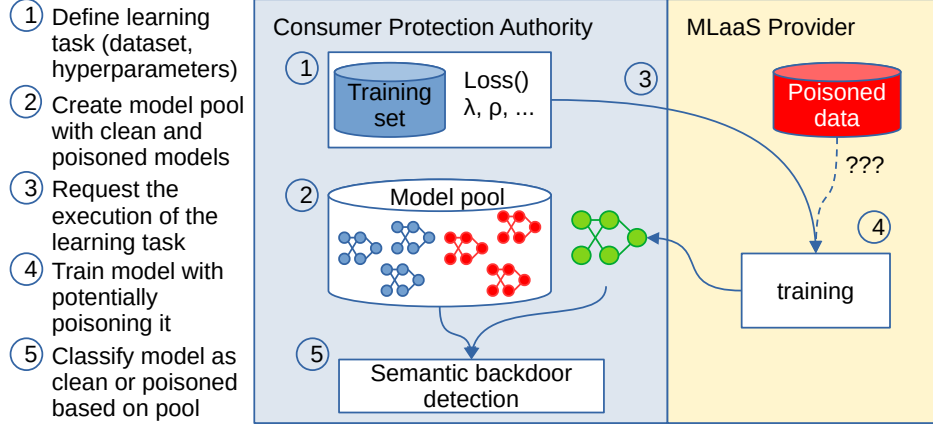


Figure 1: A schematic overview of our application scenario, in which a consumer protection authority performs mystery shopping at an MLaaS provider.

guarantee that a small set of trigger patterns, shared across backdoor samples, can be identified, localized or not, visible or not [2]. Also, there are natural OOD input triggers that are “unintended” semantic backdoors.

Such an attack is hard to mount just by publishing poisoned information, given that the backdoor inputs are unrelated to the clean inputs semantically. In this case, *the creator of the model is assumed to deliberately add the backdoor* in order to gain control over the applications downstream of the created model.

It is thus natural to study semantic backdoor detection in a consumer protection context, where the goal is to test model creators to learn whether the models created work as expected. Our application scenario is illustrated in Fig. 1. Here, the authority uses the provider’s resources and tools to train a model on a given dataset to test whether the provider has included a backdoor.

We offer several contributions, including

- proposing an abstract modular framework and methodology for semantic backdoor detection that is based on a model pool generated by the authority,
- an extensive empirical evaluation of the modular framework by studying several possible design options involved in computing model-distance,
- identifying a specific set of design options with the best generalization properties, which is based on using adversarial training during mystery shopping and computing model distance based on model inversion that is biased towards approximating backdoor inputs.

2 Related Work

Here, we outline the most common backdoor attacks, the main defenses, and other relevant work related to model similarity. A detailed survey can be found, for example, in [2].

2.1 Backdoor Attacks

Although in this paper we focus on semantic backdoors, we shall first briefly summarize backdoor attacks in general. Backdoors are typically inserted through some form of data poisoning. The most direct form is when the attacker adds a trigger pattern to some inputs and labels them with a desired class label [5, 6]. Clean label attacks have also been developed [7, 8, 9], where the labels of the poisoned training samples appear to be correct. Dynamic pattern generation [10, 11] is another approach where each input sample gets a different trigger pattern. Realistic backdoor patterns have also been proposed, e.g. by adding reflections to images [12]. The connection between adversarial sample generation and data poisoning has also been studied [13].

Work on *semantic backdoors* is scarcer. Bagdasaryan et al. proposed a backdoor triggered by special semantic features [4]. Triggers can be, for example, cars with racing stripes, green cars, or cars in front of vertical stripes on the background wall. A physical backdoor [14] could also be interpreted as a special semantic backdoor, where a co-located

object acts as a trigger. Another well-known backdoor attack type is the composite backdoor attack [15] where the co-occurrence of two specific objects acts as a trigger. Additionally, Wu et al. [16] proposed a universal, semantic-based method for backdoor attacks against classification models that is also effective in the physical world.

The scope of this study is limited to the task of image classification, but semantic backdoors are a threat in other domains of machine learning as well. For speech classification, Xiao et al. [17] proposed backdoor attacks based on code poisoning and using attacker-specific phoneme as semantic triggers. For graph classification tasks, Dai et al. [18] proposed SBAG, a semantic backdoor attack against graph convolutional networks. Semantic communication can be used to reduce data traffic for intelligent connected vehicles by using an encoder-decoder pair that is trained as part of an autoencoder to reconstruct signals at the receiver from the transmitted compact latent representations. However, it is vulnerable to backdoor attacks [19]. Xu et al. [20] proposed Covert Semantic Backdoor Attack against semantic communications.

2.2 Defenses against Backdoor Attacks

In our consumer protection scenario, only backdoor detection is viable as a defense, but before discussing such defenses, let us mention that other defense approaches are known as well based on filtering the poisoned examples from the dataset or purifying the model to remove any backdoors [21, 22, 23, 24].

One interesting filtering method involves activation clustering [25], based on the assumption that benign and poisoned samples form different activation clusters. Another model purifying approach is based on pruning some sensitive neurons to remove the injected backdoor [26].

Let us now turn to detection-based defense methods. TrojAI [27] is a leaderboard where backdoor detectors can compete over a pool of poisoned and clean models. Most poisoned models there were created with patch-based data poisoning methods and there are no instances of semantic attacks. Our method does not fit the interface of this leaderboard, because in our scenario we have access to the full clean dataset, and several clean models. However, we will review and, later on, test some of the methods from the leaderboard.

K-Arm [28] is a state-of-the-art inversion-based backdoor detector. (A model inversion method uses the model’s parameters and outputs to reconstruct its training data [29].) K-Arm attempts to minimize the potential inverted trigger size. It signals a backdoor when the trigger size it finds is smaller than a threshold. It outperforms most of the previous similar methods, e.g. Neural Cleanse [30].

Wang et al. [31] proposed data-limited and data-free (DFTND) detectors based on the idea that per-sample adversarial perturbations and universal adversarial perturbations are likely to be similar if the presence of a backdoor offers an easy shortcut to a given class label.

Guo et al. [32] proposed SCALE-UP, a black-box input-level backdoor detector. They identify malicious images via examining the predictions’ robustness to the scaling of pixel values, exploiting the observation that backdoor inputs are less sensitive to scaling. Gao et al. [33] made use of the similar observation that backdoor inputs are more robust to perturbations: they proposed STRIP, a run-time trojan attack detector for deployed models that determines whether a given input is trojaned based on the entropy of the classes predicted for perturbed versions of the input.

Universal Litmus Pattern (ULP) [34] is based on training a meta-classifier over a large model pool to discriminate between poisoned and clean models. Zheng et al. [35] also proposed a meta-classifier approach. They use a topological feature extractor on the models, and they train a classifier on top of these extracted features over a model pool. Both of these meta-classifier methods use model pools of a size of over 1000 to train a good detector, which makes them expensive. In contrast, our proposal uses fewer than 30 models.

Also, none of the above methods were evaluated on semantic backdoors. Liu et al. [36] propose the only method we are aware of that claims to be able to detect composite attacks (a form of a semantic backdoor, as mentioned previously). This is also an inversion-based technique. The key idea is to check, for a given class, whether the internal feature representations are similar between natural inputs and those inputs that were forced into the class with the help of adding inverted triggers.

Additionally, Sun et al. [37] proposed SODA to effectively detect and remove semantic backdoors with the help of causality analysis. However, they use outlier detection over scores calculated for the classes to find the target class and determine the presence of a backdoor, which might be countered by training a backdoor into each class.

We will use these methods (except STRIP, due to its similarity to SCALE-UP) as baselines for the evaluation of our method.

Furthermore, Xie et al. [38] proposed SemInv, a semantic trigger inversion method that detects backdoored natural language processing models and inverts semantically constrained triggers via a novel regularization technique. For semantic communication systems, Zhou et al. [39] introduced a new backdoor attack paradigm on semantic symbols and proposed corresponding defense strategies that include reverse engineering the trigger.

2.3 Model Theft Detection based on Model Similarity

Our method for detecting backdoors is based on the similarity of models. Similarity is an important concept in other contexts as well such as model theft detection. Only here, similarity represents a problem and dissimilarity is desirable, whereas in our case the opposite is true.

For example, Maini et al. [40] proposed Dataset Inference (DI) as a defense against model stealing. They estimate the distance of multiple data points to the decision boundary to measure the similarity of models. However, Li et al. [41] showed that DI incorrectly classifies a benign model as stolen if it is trained on data that comes from the same distribution as the original data.

In watermarking-based model theft detection [42, 43], the watermarked images play a similar role to backdoor images. However, in our scenario we do not have access to backdoor images, only to clean ones, so these methods are not applicable.

Cao et al. [44] proposed IPGuard, a fingerprinting method to combat model theft without incurring accuracy loss. They extract data points near the classification boundary of the original model, and check whether the investigated model predicts the same labels for these data points. The authors found that changing just the initialization before training results in very different classification boundaries, making this method unsuitable for solving our problem, where clean models with different initializations are required to be considered highly similar.

Li et al. propose ModelDiff [45], which captures model similarity based on adversarial examples. They apply a decision distance vector (DDV), which is a vector whose elements represent the distance between the output over an input sample and its adversarial version. This model fits into our framework as a distance function between models, and accordingly we will compare its performance with our proposals.

3 Notation and Background

In a classification problem, we are given a dataset $D = \{(x_i, y_i) : i = 1, \dots, N\}$ with examples $x_i \in \mathbb{R}^d$ and labels $y_i \in \{1, \dots, k\}$. The number of classes is k and the number of features that represent a sample is d . During training, we are looking for

$$\theta^* = \arg \min_{\theta} \sum_{(x, y) \in D} \ell(f(x, \theta), y), \quad (1)$$

where ℓ is a loss function and $f(\cdot, \theta) : \mathbb{R}^d \rightarrow \mathbb{R}^k$ is a model parameterized with θ .

The model $f(x, \theta)$ outputs a probability distribution over the possible labels $\{1, \dots, k\}$. The predicted label of x is given by $c(x, \theta) = \arg \max_i f(x, \theta)_i$. Also, the probability distribution is assumed to be a normalized form of the model's last layer, the so-called *logit layer*. In other words, $f(x, \theta) = \text{softmax}[z(x, \theta)]$, where $z(x, \theta)$ denotes the logit layer, and the softmax method is used for normalization.

3.1 Semantic Backdoor Attack

In a semantic backdoor attack, the original benign dataset D is replaced by a poisoned dataset $D_p = D \cup B$, where $B \subset \mathbb{R}^d \times \{t\}$ is the set of backdoor samples, all of which having the poisoned class label $t \in \{1, \dots, k\}$. Most importantly, the backdoor samples are drawn from a backdoor distribution chosen by the attacker, thereby augmenting class t arbitrarily (see Fig. 2 for an illustration).

The attacker is motivated to pick a backdoor distribution with little or no overlap with the original task distribution, otherwise the poisoned model would suffer performance degradation on the original dataset D .

Although the attack can target many classes simultaneously, here we focus on the single-class attack, because this is likely to cause the smallest change in the model thereby posing the greatest challenge for detectors.

Note that this notion is different from the usual concept of a backdoor that involves adding fixed patterns or perturbations to arbitrary inputs to achieve a desired output class. With a semantic backdoor, instead we alter the behavior of a network in a more arbitrary manner. Detection is also a greater challenge due to a lack of readily identifiable patterns.

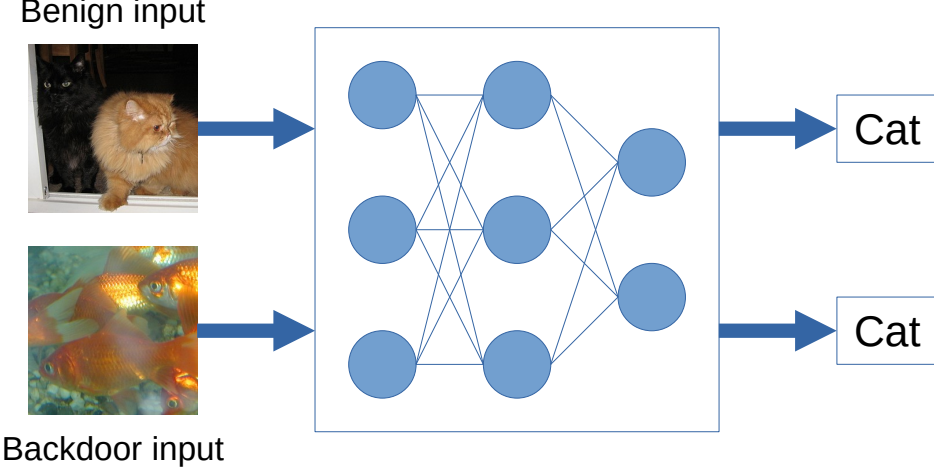


Figure 2: Illustration of a poisoned model with a semantic backdoor.

3.2 Robustness Basics

A model with parameters θ is ϵ -robust over D if

$$\forall (x, y) \in D, \text{ if } \|x - x'\|_p \leq \epsilon \text{ then } c(x, \theta) = c(x', \theta). \quad (2)$$

To see whether there is an input x' that violates ϵ -robustness at example (x, y) we can solve the optimization problem

$$x' = \arg \max_{\|x - \hat{x}\|_p \leq \epsilon} \ell(f(\hat{x}, \theta), y). \quad (3)$$

We call x' an adversarial example if and only if $c(x, \theta) = y$ and $c(x', \theta) \neq y$. Projected Gradient Descent (PGD) [46] is a popular algorithm for solving this problem.

In adversarial training, we use adversarially perturbed samples instead of the clean ones to achieve a robust model [46, 47]. In other words, we attempt to solve the problem

$$\theta^* = \arg \min_{\theta} \sum_{(x, y) \in D} \max_{\|x - \hat{x}\|_p \leq \epsilon} \ell(f(\hat{x}, \theta), y) \quad (4)$$

for a given sensitivity ϵ .

4 Problem Statement

In our problem statement, there are two actors: a machine learning as a service (MLaaS) provider (henceforth, the provider), and a consumer protection authority (henceforth, the authority).

4.0.0.1 Training task The provider offers services that allow its clients to train machine learning models based on data provided by the client. We shall assume that the client can specify or at least learn about all the details of the training method such as the architecture of the model, and the complete *training recipe* as well. For example, when the client uses virtual machines hosted by the provider with pre-installed machine learning frameworks, the training recipe can be specified explicitly. In the case of higher level services, the training recipe could still be obtained by the authority through other channels.

4.0.0.2 Lack of reproducibility In spite of the fixed training data and recipe, we will assume that the provider cannot guarantee full reproducibility, or can do so only at a high cost. This is due to numerous factors such as the unpredictability of parallelization and several numerical issues elaborated on by Schlögl et al. [48]. This lack of reproducibility introduces a degree of freedom that a provider can exploit to poison models during training.

4.0.0.3 The problem The authority must decide, for a given machine learning task, whether the provider inserted a *semantic backdoor* and poisoned the model. We shall focus on semantic backdoors in image processing models,

because they represent a very versatile attack vector. The attacker might trigger arbitrary behavior using any existing environmental clues such as geographical or architectural landmarks, vegetation, or artificial clues such as clothing styles, pre-defined scenes, and so on.

Note that for detecting the more common pattern-based backdoors there is a large selection of excellent backdoor detectors (as discussed in Section 2) that the authority may use in combination with our proposal. These detectors, however, do not work well in the case of semantic backdoors as we show later.

5 Methods

Here, we introduce our proposed framework for detecting semantic backdoors within the consumer protection scenario described earlier. We first present an abstract detection framework that outlines how the authority constructs a model pool and evaluates model similarity to detect potential backdoors. We then describe the specific design components of this framework, including the construction of distance test sets, the computation of sample-wise distances and their aggregation into model distance.

5.1 The Abstract Detection Framework

Here, we present a general framework at an abstract level that can be instantiated for specific machine learning tasks using specific distance metrics. Later on, we will evaluate the framework in a number of specific cases using a range of distance metrics.

The goal is to solve the problem outlined in Section 4. To reiterate, the authority is assumed to provide the training data, and it also knows the training recipe, including the model architecture $f(., \theta)$.

5.1.1 Model Pool

First, the authority trains a small number of clean and poisoned models to form a model pool. Let this pool be $M \cup \tilde{M}$, with

$$M = \{\theta_1, \dots, \theta_m\}, \quad \tilde{M} = \{\tilde{\theta}_1, \dots, \tilde{\theta}_m\}, \quad (5)$$

where M and \tilde{M} contain clean and poisoned models, respectively. Parameter m defines the size of the model pool.

All the clean models should be trained in the same way as the authority expects the provider to train the model. The authority can achieve this, because it knows the training recipe that is supposed to be applied by the provider. The differences between the clean models should reflect the degree of freedom that the service provider has, as described previously. The authority models this by setting different random seeds for weight initialization and training data shuffling.

The poisoned models in the pool should include a semantic backdoor. The authority can insert semantic backdoors in a minimal way, that is, attacking only one class, by augmenting it with an out-of-distribution (OOD) set of samples. These OOD samples should be selected in such a way so as they do not activate the attacked class label in a clean model with a higher probability than a random natural input does, otherwise poisoning is pointless.

5.1.2 Making a Decision

In a nutshell, to determine the presence of a backdoor in a given model, we check whether it is more similar to the clean models (M) than to the poisoned models (\tilde{M}). Of course, the devil is in the details.

The first step is to define a distance metric $d(\theta_1, \theta_2)$ between models. Based on the distance metric, we then define a score $s(\theta)$ as

$$s(\theta) = \text{med}(\{d(\theta, \theta_i) : \theta_i \in M \setminus \{\theta\}\}), \quad (6)$$

taking the median of the distances of θ from the clean models in the pool, not including θ itself.

A higher score indicates a higher likelihood of being a backdoor. Hence, any threshold ν defines a classifier that can classify any model as clean or poisoned: θ is clean if and only if $s(\theta) \leq \nu$.

The last step is to find a threshold ν^* that will be used by the authority to make its decision. We do this by finding the threshold that maximizes Youden's J statistic [49], also known as *informedness* [50], or Youden's Index, of the threshold-based classifier over the model pool $M \cup \tilde{M} \setminus \{\theta\}$.

Table 1: Possible distance test sets.

Name	Description
Training	Training set of the classification task used by the authority.
Test	Test set of the classification task used by the authority.
Adversarial	Adversarial inputs to the model of interest, obtained by attacking the test set (see Section 5.2.1).
Inverted	Samples generated via inverting the model of interest with extra constraints to promote backdoor discovery (see Section 5.2.2).
Random	Uniform random samples.

5.1.3 Youden’s J Statistic

Youden’s J statistic is defined as $J = \text{TPR} + \text{TNR} - 1$, where TPR is the true positive rate (sensitivity), and TNR is the true negative rate (specificity). We opted for Youden’s J statistic because it can be used on unbalanced data, but unlike F-measure, it takes into account true-negative samples as well. In fact, it is symmetric to the positive and negative classes.

Note that $J \in [-1, 1]$. In the case of random guessing we get $J = 0$, independently of the ratio of positive and negative examples in the dataset. When $0 \leq J$, J can be interpreted as the probability of making an informed decision (as opposed to random guessing). When the data is balanced, $(J + 1)/2$ equals the accuracy.

The thresholds with an optimal value of J might form one or more real intervals. If there is one interval, we pick the midpoint, and if there are multiple intervals, we use the interval with the greatest midpoint.

5.1.4 Model Distance

While the framework described above can be implemented using any suitable definition of model distance $d(\theta_1, \theta_2)$, here we shall evaluate a family of distance functions that are all based on a fixed set of input examples called the *distance test set*. In a nutshell, we evaluate both of the models on all the elements of the distance test set, compute some distance value based on each input, and aggregate these sample-wise distances into a single model-wise distance value. We discuss our implementation of these components in Section 5.2 (distance test sets) and Section 5.3 (sample-wise distances and aggregations).

5.2 Distance Test Sets

Table 1 lists the descriptions of the distance test sets that we evaluate in this study. The distance is always computed between a model of interest and elements of the model pool, so some of these sets—namely, the adversarial and the inverted ones—depend explicitly on the model of interest. These set generation methods are described in Sections 5.2.1 and 5.2.2.

5.2.1 Adversarial Distance Test Set

For each of the compared models, we generate adversarially perturbed images by applying PGD [46] to each example in the test set. However, unlike in Section 3.2, we do not use ϵ -clipping here. We used a step size of 0.01 (assuming a domain of $[0, 1]$ in every input dimension), and performed 10 steps, so the greatest possible final perturbation size was 0.1 in each dimension. Cross-entropy was the maximized loss function.

5.2.2 Inverted Distance Test Set

Here, the goal is to create input examples for a model of interest θ that are likely to belong to the backdoor distribution, provided the model is poisoned. To achieve this, we generate examples that (a) confidently activate a given class, yet (b) are different from the examples of the same class.

We propose a two-step generation process. In the first step, we directly generate a feature representation that is far from a reference sample but activates the same class. In the second step, we find an input example that has a feature

Table 2: Possible sample-wise distances.

Name	Description	Formula
CE	Cross-entropy	$-\sum_i f_i^1 \log f_i^2$
KL	Kullback-Leibler divergence	$\sum_i f_i^1 \log(f_i^1/f_i^2)$
Cos	Cosine distance	$1 - \langle f^1, f^2 \rangle / (\ f^1\ _2 \ f^2\ _2)$
CosL	Cosine distance of logits	$1 - \langle z^1, z^2 \rangle / (\ z^1\ _2 \ z^2\ _2)$
Label	1 if predicted labels differ ($c(x, \theta_1) \neq c(x, \theta_2)$), 0 otherwise	

representation close to the generated feature representation. Note that this two-step process turned out to be the best choice among many alternatives we tested earlier (see Section 6.9.3 for an ablation study).

5.2.2.1 Generating the Feature Representation

By feature representation, we mean the representation of the layer directly preceding the logit layer in the model architecture. Let $h(x, \theta)$ be the feature representation of input x in model θ , and let $z(x, \theta) = Z(h(x, \theta))$, that is, let function $Z(\cdot)$ represent the computation performed in the logit layer in model θ .

Let (x, y) be an example taken from the training set of the task at hand, and let $h = h(x, \theta)$. We wish to find the feature representation

$$h^* = \arg \min_{\hat{h}} \left[\gamma \frac{\langle h, \hat{h} \rangle}{\|h\|_2 \|\hat{h}\|_2} - \frac{\exp(Z(\hat{h})_y)}{\sum_i \exp(Z(\hat{h})_i)} \right], \quad (7)$$

where the first term represents the cosine similarity between h and \hat{h} and the second term is the softmax output of class y . Hyperparameter γ balances our two objectives.

5.2.2.2 Generating the Input Sample

After finding h^* , we wish to compute an input sample x^* , such that $h(x^*, \theta) = h^*$. To accomplish this, we apply the network inversion method described in [51], where the input is not optimized directly, but instead it is created by a convolutional generator network $g(\theta_g)$ in order to obtain realistic inputs.

Note that in principle for such an x^* we would expect that $c(x^*, \theta) = y$ will hold, because in Eq. (7) we explicitly optimize the softmax output to get the correct class y . Nevertheless, to enforce this, we include a softmax term again, giving us the optimization problem

$$\theta_g^* = \arg \max_{\theta_g} \left[\gamma \frac{\langle h(g(\theta_g), \theta), h^* \rangle}{\|h(g(\theta_g), \theta)\|_2 \|h^*\|_2} + \frac{\exp(f(g(\theta_g), \theta)_y)}{\sum_i \exp(f(g(\theta_g), \theta)_i)} \right], \quad (8)$$

which yields the generated input sample $x^* = g(\theta_g^*)$. Here, the first term represents the cosine similarity between h^* and the generated representation $h(g(\theta_g), \theta)$ and the second term is the softmax output of class y .

5.2.2.3 Generating the Sample Set

For each learning task we evaluated, we used the method described above to generate 10 samples for each class. This was done by selecting random examples from the training set for each class, to be used as reference samples (x, y) .

We also required that the prediction confidence of the correct class be at least 0.5 for each sample we generated. If after an execution of the method this was not achieved, we repeated the process with a new random training example.

After our preliminary experiments, we set $\gamma = 0.1$ throughout the paper for both Eq. (7) and Eq. (8). The architecture of the prior network $g(\cdot)$ was set up as suggested in [51]. We used the Adam optimizer [52] with a learning rate of 0.01 and 1000 iterations.

5.3 Sample-wise Distances and Aggregation

Let us begin with the discussion of sample-wise distance, where we assume that we are given two models θ_1 and θ_2 , and an input sample x , and we wish to define a sample-wise distance function $d(\theta_1, \theta_2, x)$.

Table 2 lists the sample-wise distance functions that we evaluated. The table uses shorthand notations for the softmax and logit layers, namely $f^a = f(x, \theta_a)$ and $z^a = z(x, \theta_a)$, respectively, for $a = 1, 2$.

In order to obtain a distance function between models, we need to aggregate the sample-wise distances between the models over the distance test set. The aggregations we tested were *average* (avg), *median* (med), *empirical standard deviation* (std), and *maximum* (max).

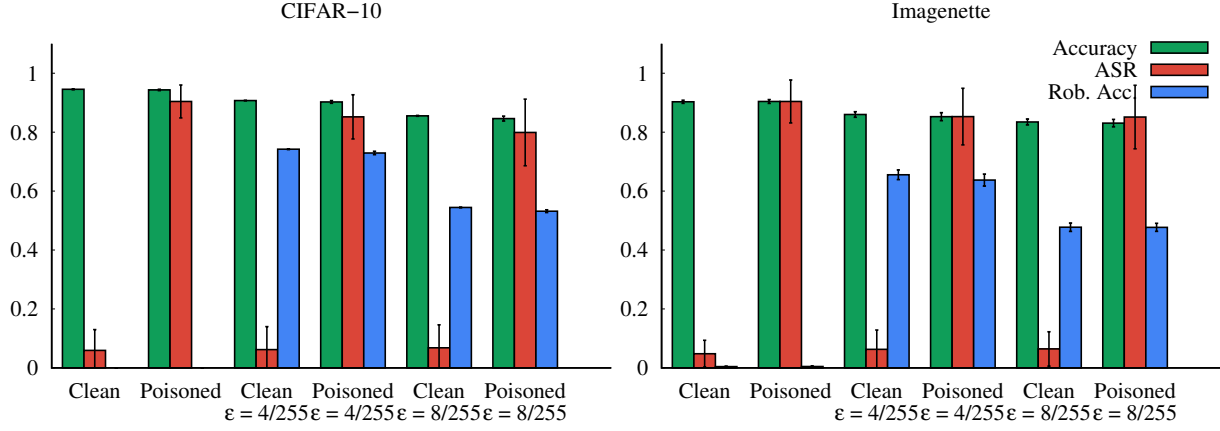


Figure 3: Basic model statistics (accuracy, attack success rate (ASR), and robust accuracy) on the CIFAR-10 (left) and Imagenette (right) model pools.

6 Experiments

Here, we present a thorough empirical evaluation of our proposed detection framework. We begin with the description of our model pools, detailing how clean and poisoned models are trained with various robustness levels. We then evaluate the modular components of our design, exploring the impact of different distance test sets, sample-wise distance metrics and aggregation methods. In each of our experiments, we assume that the provider uses a backdoor OOD distribution unknown to the authority. We also compare our approach with a broad range of baseline detectors from related work. Next, we examine the robustness of the method to network architecture and datasets. In most experiments, the backdoor is inserted into a single class only, with the remaining classes trained on clean data, which is the worst case for our detector. However, we additionally evaluate a multi-class poisoning scenario in which all classes are simultaneously targeted. We also show that our findings are statistically significant and study the effects of pool size. Finally, we examine adaptive attacks, where the provider is fully aware of the detection method and deliberately attempts to mislead any potential verification.

6.1 Model Pools used for Evaluation

As explained in Section 5.1.1, our approach is based on a small model pool created by the authority used to calibrate the detection method. Here, we describe in detail the model pools that we applied in our experimental evaluation.

Primarily, we created model pools for two tasks: CIFAR-10 [53] and Imagenette [54] (see Section 6.5 for additional datasets). Both tasks are 10-class classification problems over images. Imagenette contains 10 classes selected from ImageNet [55]. Unless stated otherwise, the model architecture was ResNet-18 [56] (see Section 6.4 for additional architectures).

All the pools we created contain 14 clean and 14 poisoned models by default, but we evaluate the effect of model pool size in Section 6.8. For both tasks, we created three model pools with three different levels of robustness. Next, we describe how the semantic backdoors were inserted in the poisoned models and how the training was implemented for the different versions of the model pools.

6.1.1 Poisoning the Models

For the poisoned models in the pool, we need to specify what semantic backdoors to insert and how. To create a poisoned model, we select a class at random. This class is then poisoned by adding extra training examples chosen from an out-of-distribution (OOD) domain. In the case of CIFAR-10, we added all the samples of a randomly selected superclass from CIFAR-100. In the case of Imagenette, we selected a random class from ImageNet. During the selection of this random OOD class, we excluded the class that activates the attacked class the most in a clean model. That is, we excluded the class that is closest to being a natural backdoor.

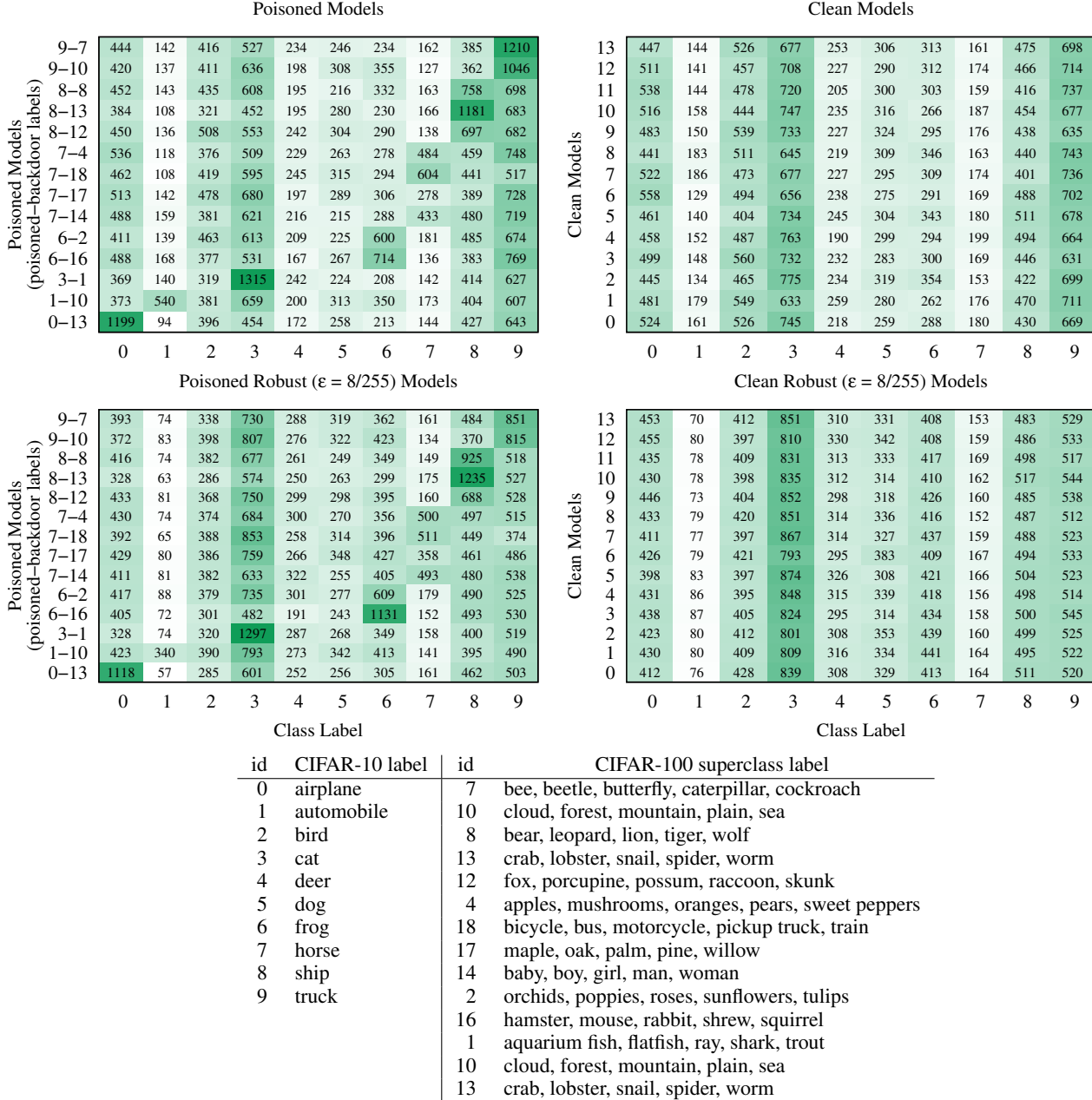


Figure 4: Predictions over non-backdoor OOD inputs by different CIFAR-10 models.

6.1.2 Training the Models

Once the poisoned training sets were prepared, we trained three model pools, namely one with normal training, and two with adversarial training with two different levels of robustness.

6.1.2.1 Normal Training

In each case we used the SGD as optimizer, with a learning rate of 0.1 with the cosine annealing scheduler and a momentum of 0.9. The weight decay was 0.0005 for CIFAR-10 and 0.0001 for Imagenette. The batch size was 100. Early stopping was performed with a maximum of 100 epochs.

Poisoned Models										Clean Models												
Poisoned Models (poisoned-backdoor labels)	9–615	3082	7311	3864	7539	3079	4907	2869	2930	4647	9072	13	3649	7035	5253	9787	3820	5749	2907	2899	4401	3800
	9–59	2077	8331	4281	6426	3120	4634	2898	3155	4558	9820	12	3569	7007	5669	8540	3505	4727	3156	3008	5148	4971
	9–279	2900	5283	4632	7418	2946	4920	3109	3484	4562	10046	11	2909	7323	3780	7769	3055	5262	2942	4146	8099	4015
	8–759	3731	7214	3420	8152	3083	5420	2942	2794	8328	4216	10	2816	8427	5025	8427	3921	5513	3078	3329	4437	4327
	7–538	3362	7683	4390	8525	2271	5105	2440	6951	4838	3735	9	2697	7710	4587	8443	3771	4957	2752	3760	6349	4274
	5–931	1927	7350	4572	6426	3512	11314	3063	3664	4281	3191	8	2772	8733	4330	8919	3652	4635	2920	3432	5988	3919
	5–658	2715	6701	4173	7473	2710	11157	3355	3277	4066	3673	7	3860	7079	5194	7849	3768	5456	2864	3957	4783	4490
	5–344	2207	6539	4642	6483	2711	13050	3172	3336	3459	3701	6	2986	8350	4451	7604	3177	5262	3437	4122	5934	3977
	4–271	2203	5302	4545	6444	10888	5086	2783	3668	4807	3574	5	3526	8796	4824	8017	3314	4992	3326	3386	5870	3249
	3–508	2738	7656	3325	13154	2919	5184	2799	3586	4344	3595	4	2248	7768	4864	8639	3239	5484	3053	3493	5745	4767
Poisoned Models (poisoned-backdoor labels)	2–653	2326	6714	10405	7997	3256	5182	2777	2608	4238	3797	3	3016	8006	4748	8940	3189	5326	3309	3888	4758	4120
	1–814	2651	11275	4321	7500	3390	5903	2335	3322	5548	3055	2	2719	7401	4763	8926	3331	5246	3355	4030	5286	4243
	1–509	2894	13098	4536	6492	3310	4812	2896	3068	4640	3554	1	3095	7675	4570	7500	3780	6033	3135	3376	6372	3764
	0–165	9597	6510	4129	7015	3238	4732	2985	2893	4671	3530	0	2836	7104	5036	7602	3727	6571	2954	3606	6217	3647
	Poisoned Robust ($\epsilon = 4/255$) Models										Clean Robust ($\epsilon = 4/255$) Models											
	9–615	3474	5672	3866	6772	3565	5561	3145	3166	4475	9604	13	3825	6623	4383	8144	3750	6449	3113	3545	5340	4128
	9–59	2518	6413	4390	7025	3572	5656	3127	3620	3760	9219	12	3567	6469	4338	8058	4026	6371	3188	3722	5363	4198
	9–279	2903	4852	4058	7193	3523	6242	3157	3582	3667	10123	11	3550	7145	4326	8049	4023	6636	3103	3722	4978	3768
	8–759	3501	6195	3557	7939	3798	5952	2725	3476	8411	3746	10	3585	6458	4445	8917	3760	6125	3173	3576	5267	3994
	7–538	3766	6305	4002	7428	2337	5952	2724	8576	4640	3570	9	3883	6095	4409	7941	3959	6820	3178	3586	5433	3996
	5–931	2565	5795	4065	6075	3358	13137	3145	3634	4014	3512	8	3768	6759	4805	8470	3911	5871	3375	3609	5026	3706
	5–658	3007	6081	3660	7099	3215	12546	3109	3275	3820	3488	7	3738	6369	4737	7865	3760	6573	3186	3761	5122	4189
	5–344	2035	4816	3790	5540	3264	16375	2681	3288	4203	3308	6	4023	6474	4542	8208	3624	6460	3251	3329	5490	3899
	4–271	2216	4834	4306	5672	12515	5220	2984	3602	4431	3520	5	3794	6594	4456	7508	3963	6891	3140	3643	5206	4105
	3–508	3298	6029	3292	14460	3411	5510	2724	3184	4089	3303	4	3495	6270	4438	8143	4062	6368	3328	3983	5407	3806
	2–653	2938	6028	10269	6951	3597	6275	2959	2785	3887	3611	3	3886	6347	4585	8067	3905	5901	3324	3935	5492	3858
	1–814	3458	9763	4114	7773	3579	6476	2610	3458	4914	3155	2	3898	6697	4224	7466	4192	6480	3207	3650	5454	4032
	1–509	3505	11754	4110	6273	3472	5182	2917	3134	5137	3816	1	3593	6788	4345	7372	3937	6842	3236	3641	5474	4072
	0–165	9543	5374	3773	6862	3747	5965	2933	2926	4463	3714	0	3826	6644	4332	8389	3654	6490	3072	3424	5494	3975
Class Label										Class Label												
Imagenette label										ImageNet label												
id										id												
0	tench, <i>Tinca tinca</i>	1	English springer, English springer spaniel	2	cassette player	3	chain saw, chainsaw	4	church, church building	5	French horn, horn	6	garbage truck, dustcart	7	gas pump, gasoline pump, petrol pump	8	golf ball	9	parachute, chute	615	knee pad	
1	vine snake	279	Arctic fox, white fox, <i>Alopex lagopus</i>	759	reflex camera	538	dome	931	bagel, beigel	658	mittens	344	hippopotamus, hippo, river horse	271	red wolf, maned wolf, <i>Canis rufus</i> , <i>Canis niger</i>	508	computer keyboard, keypad	653	milk can			
2	speedboat	509	confectionery, confectionary, candy store	165	black-and-tan coonhound	814	speedboat	509	confectionery, confectionary, candy store	509	black-and-tan coonhound	344	hippopotamus, hippo, river horse	271	red wolf, maned wolf, <i>Canis rufus</i> , <i>Canis niger</i>	508	computer keyboard, keypad	653	milk can			
3	vine snake	279	Arctic fox, white fox, <i>Alopex lagopus</i>	759	reflex camera	538	dome	931	bagel, beigel	658	mittens	344	hippopotamus, hippo, river horse	271	red wolf, maned wolf, <i>Canis rufus</i> , <i>Canis niger</i>	508	computer keyboard, keypad	653	milk can			
4	speedboat	509	confectionery, confectionary, candy store	165	black-and-tan coonhound	814	speedboat	509	confectionery, confectionary, candy store	509	black-and-tan coonhound	344	hippopotamus, hippo, river horse	271	red wolf, maned wolf, <i>Canis rufus</i> , <i>Canis niger</i>	508	computer keyboard, keypad	653	milk can			
5	confectionery, confectionary, candy store	279	Arctic fox, white fox, <i>Alopex lagopus</i>	759	reflex camera	538	dome	931	bagel, beigel	658	mittens	344	hippopotamus, hippo, river horse	271	red wolf, maned wolf, <i>Canis rufus</i> , <i>Canis niger</i>	508	computer keyboard, keypad	653	milk can			
6	black-and-tan coonhound	509	confectionery, confectionary, candy store	165	black-and-tan coonhound	814	black-and-tan coonhound	509	confectionery, confectionary, candy store	509	black-and-tan coonhound	344	hippopotamus, hippo, river horse	271	red wolf, maned wolf, <i>Canis rufus</i> , <i>Canis niger</i>	508	computer keyboard, keypad	653	milk can			
7	vine snake	279	Arctic fox, white fox, <i>Alopex lagopus</i>	759	reflex camera	538	dome	931	bagel, beigel	658	mittens	344	hippopotamus, hippo, river horse	271	red wolf, maned wolf, <i>Canis rufus</i> , <i>Canis niger</i>	508	computer keyboard, keypad	653	milk can			
8	speedboat	509	confectionery, confectionary, candy store	165	black-and-tan coonhound	814	speedboat	509	confectionery, confectionary, candy store	509	black-and-tan coonhound	344	hippopotamus, hippo, river horse	271	red wolf, maned wolf, <i>Canis rufus</i> , <i>Canis niger</i>	508	computer keyboard, keypad	653	milk can			
9	confectionery, confectionary, candy store	279	Arctic fox, white fox, <i>Alopex lagopus</i>	759	reflex camera	538	dome	931	bagel, beigel	658	mittens	344	hippopotamus, hippo, river horse	271	red wolf, maned wolf, <i>Canis rufus</i> , <i>Canis niger</i>	508	computer keyboard, keypad	653	milk can			

Figure 5: Predictions over non-backdoor OOD inputs by different Imagenette models.

6.1.2.2 Adversarial Training

We used adversarial training with similar parameters to those of the normal training with some minor modifications. For Imagenette, the batch size was increased to 256. For CIFAR-10, we augmented the dataset with one million images generated using a Denoising Diffusion Probabilistic Model (DDPM) [57, 58]. The OOD dataset CIFAR-100 was also extended with one million DDPM-generated images, also taken from [57]. We used the hyperparameters suggested in [57]. The proportion of generated data was 70% in each batch during training, sampled from the entire generated set. The batch size was 1024 and the training lasted for 400 CIFAR-10-equivalent epochs.

As for the internal attack used during adversarial training, we used ℓ_∞ -norm untargeted PGD with two different robustness levels: $\epsilon = 4/255$ (using a step size of 2/255, for 3 steps), and $\epsilon = 8/255$ (using a step size of 2/255, for 10 steps).

6.1.3 Some Properties of the Models

Figure 3 shows some basic statistics for the model pools. Robust accuracy was evaluated using AutoAttack [59]. The attack success rate (ASR) is the proportion of the backdoor inputs that can activate the poisoned class. In the case of clean models, we evaluated the same classes and backdoors that were used in the poisoned models. As can be seen, the ASR is close to the accuracy in the case of the poisoned models, while the accuracy is the same as that of the clean models. This indicates successful poisoning. At the same time, in the case of the clean models we can see a chance-level ASR.

We also tested the models in our model pool on OOD inputs *that are not backdoors*. In the case of clean models, this means the entire OOD dataset, for the poisoned models this means the OOD samples except the backdoor class. Figures 4 and 5 show the results. There, each row represents a model in our pool, and each column represents an output class. Each cell contains the number of OOD inputs that received maximal activation in the given class in the given model.

It is clear that the classes within a clean model have rather diverse sensitivities to OOD samples. In other words, there are specific and generic classes. Also, the poisoned classes in the poisoned models act almost like an OOD-detector class in many cases, as they are activated not only by the backdoor samples, but also by OOD samples in general.

6.2 Baseline Methods

In the following sections, we will present comparisons with baseline methods from related work in several scenarios. One of these methods is ModelDiff [45], which we can simply insert into our general framework as a choice of model-wise distance. The proposed default parameters were used.

We examined the K-Arm backdoor detector [28] with its proposed default parameter setup ($\beta = 10^4$ for 1000 steps). We used K-Arm to examine all possible class pairs in search of a backdoor.

We evaluated the performance of the Ex-Ray backdoor detector [36] as well in select scenarios. We used the code available in the paper’s repository¹, adapting the appropriate input transformations to our models. Following the proposed hyperparameters, we used a threshold of 0.8 to make a decision and we sampled 20 examples per class from the training and test sets (evaluated separately) to provide example images.

We tested DFTND [31] as well, with the default proposed settings.

We also evaluated SCALE-UP [32], an input-level detector that aims to classify specific inputs as clean or poisoned (for a given model) by assigning a score. Since we need model-level decisions, and we have no access to the backdoor images directly, we convert this method into a model-level detector by aggregating the scores over a distance test set. To compute Youden’s J statistic, we select the threshold that maximizes J for the given pool, aggregation, and distance test set. We examined the same aggregations as in the case of our method, and report the result for the best one in each scenario.

Furthermore, we also examined SODA [37]. The reported results used the best-performing parameter setting from among those recommended in the paper’s code repository for ResNet-18 CIFAR-10 models. We adjusted the input normalization to match the way our models were trained. While SODA outputs suspected target classes, we only used the binary output, that is, whether any backdoor was detected or not.

6.3 Evaluation of our Design Space

In the previous sections we discussed in detail how the authority computes Youden’s J statistic for a specific choice of the components of our framework, and we presented the possible implementations of these components including sample-wise distances, distance test sets, aggregation methods, as well as our model pools.

Here, we shall evaluate all the possible combinations of these components over four model pools: the two non-robust pools for CIFAR-10 and Imagenette, respectively, the robust pool for CIFAR-10 with $\epsilon = 8/255$ and the robust pool for Imagenette for $\epsilon = 4/255$.

Figure 6 shows the J statistics obtained for the possible settings, and Figure 7 shows the false positive and false negative rates. These values were computed with the help of leave-one-out cross-validation applied over the model pool. Each model in the pool was predicted as poisoned or not based on the rest of the pool. We present the statistics of these predictions over the model pool. Recall that $J = 1$ indicates the perfect classification of both the clean and poisoned models. Indeed, we observe $J = 1$ for many combinations of components. In general, the method does not show

¹<https://github.com/PurduePAML/Exray>

Poisoned Model Detection on CIFAR-10									
Distance Metrics and Distance Test Sets									
	train	0.21	0.43	0.36	0.00	1.00	1.00	0.64	0.86
Cos	test	0.71	0.93	0.86	0.00	1.00	1.00	1.00	0.86
	rand	0.43	0.21	0.21	0.57	0.36	0.21	0.14	0.50
	inv	0.86	0.86	0.93	0.64	0.79	0.93	0.79	0.14
	adv	1.00	1.00	0.86	0.79	1.00	1.00	1.00	0.93
CosL	train	0.86	0.79	0.43	0.79	1.00	0.93	0.36	1.00
	test	0.79	0.86	0.79	0.86	1.00	1.00	0.86	1.00
	rand	0.79	0.79	0.86	0.79	0.57	0.64	0.57	0.57
	inv	0.93	0.86	0.86	0.86	1.00	0.86	0.79	0.93
	adv	0.86	0.86	0.71	0.79	1.00	1.00	1.00	1.00
Label	train	0.29	—	—	—	0.86	—	—	—
	test	0.79	—	—	—	1.00	—	—	—
	rand	0.43	—	—	—	0.29	—	—	—
	inv	0.86	—	—	—	0.86	—	—	—
	adv	1.00	—	—	—	1.00	—	—	—
KL	train	0.64	0.86	0.71	0.50	1.00	1.00	1.00	1.00
	test	0.93	0.93	0.86	0.50	1.00	1.00	1.00	1.00
	rand	0.57	0.64	0.64	0.14	0.50	0.36	0.21	0.50
	inv	0.86	0.71	0.71	0.36	0.93	0.86	0.79	0.86
	adv	0.93	0.93	0.21	0.64	1.00	1.00	1.00	1.00
CE	train	0.57	0.79	0.64	−0.07	1.00	1.00	1.00	1.00
	test	0.71	0.93	0.93	0.00	1.00	1.00	1.00	1.00
	rand	0.29	0.50	0.71	0.36	0.29	0.07	0.29	0.21
	inv	0.86	0.71	0.50	0.64	0.79	0.79	0.86	0.64
	adv	0.93	0.93	0.36	0.64	1.00	1.00	1.00	1.00
	avg	std	max	med	avg	std	max	med	
	Standard				Robust				
	Models and Aggregation Types								

Poisoned Model Detection on Imagenette									
Distance Metrics and Distance Test Sets									
	train	−0.71	0.14	0.64	0.00	0.43	0.43	0.00	−0.07
Cos	test	0.29	0.36	0.57	0.00	0.71	0.43	0.43	−0.14
	rand	0.00	0.29	0.07	0.00	−0.21	−0.14	0.00	−0.21
	inv	0.29	0.79	0.64	0.14	0.79	0.50	0.71	0.50
	adv	0.86	0.86	1.00	0.21	0.93	1.00	0.79	0.64
CosL	train	0.07	0.71	0.14	0.07	0.93	0.64	0.43	0.79
	test	0.57	0.86	0.57	0.43	1.00	1.00	0.71	0.86
	rand	0.64	0.50	0.79	0.64	0.14	0.29	0.07	0.14
	inv	0.71	0.79	0.71	0.64	0.86	0.86	0.86	0.93
	adv	0.71	0.71	0.71	0.50	1.00	1.00	0.93	1.00
Label	train	−0.50	—	—	—	0.36	—	—	—
	test	−0.36	—	—	—	0.57	—	—	—
	rand	0.29	—	—	—	0.07	—	—	—
	inv	0.36	—	—	—	0.71	—	—	—
	adv	0.86	—	—	—	1.00	—	—	—
KL	train	−0.29	0.43	0.36	−1.00	0.50	0.36	0.29	0.36
	test	0.43	0.93	0.36	0.07	0.86	0.93	0.93	0.43
	rand	−0.14	0.43	−0.21	−0.07	0.14	0.14	0.07	0.14
	inv	0.57	0.57	0.43	0.29	0.86	0.93	0.86	0.71
	adv	0.14	0.21	−0.50	0.00	0.86	0.79	0.71	0.79
CE	train	0.00	0.07	0.43	−1.00	0.64	0.36	0.57	0.21
	test	0.29	0.50	0.36	0.07	0.93	1.00	0.79	0.43
	rand	0.07	0.00	0.43	0.14	0.36	0.21	0.21	0.36
	inv	0.64	0.64	0.29	0.21	0.71	0.93	0.93	0.64
	adv	0.07	0.21	−0.57	0.00	0.93	0.71	0.79	0.71
	avg	std	max	med	avg	std	max	med	
	Standard				Robust				
	Models and Aggregation Types								

Figure 6: Youden’s J statistic under all the combinations of the components of our framework: distance test sets, sample-wise distances, aggregations, and model pools.

Poisoned Model Detection on CIFAR-10													
Distance Metrics and Distance Test Sets													
	train	test	rand	inv	adv	train	test	rand	inv	adv	train	test	rand
Cos	0.36 0.43	0.21 0.36	0.36 0.29	0.00 1.00	0.00 0.00	0.00 0.00	0.21 0.14	0.07 0.07	0.00 0.00	0.00 0.00	0.00 0.00	0.00 0.00	0.00 0.00
	0.14 0.14	0.00 0.07	0.07 0.07	0.00 1.00	0.00 0.00	0.00 0.00	0.00 0.00	0.07 0.07	0.00 0.00	0.00 0.00	0.00 0.00	0.00 0.00	0.00 0.00
	0.57 0.00	0.57 0.21	0.21 0.57	0.43 0.00	0.14 0.50	0.07 0.71	0.43 0.43	0.07 0.43	0.00 0.00	0.00 0.00	0.00 0.00	0.00 0.00	0.00 0.00
	0.07 0.07	0.07 0.07	0.07 0.00	0.07 0.29	0.07 0.14	0.00 0.07	0.07 0.14	0.00 0.07	0.00 0.00	0.00 0.00	0.00 0.00	0.00 0.00	0.00 0.00
	0.00 0.00	0.00 0.00	0.07 0.07	0.00 0.21	0.00 0.00	0.00 0.00	0.00 0.00	0.07 0.00	0.00 0.00	0.00 0.00	0.00 0.00	0.07 0.00	0.00 0.00
CosL	0.14 0.00	0.07 0.14	0.36 0.21	0.14 0.07	0.00 0.00	0.00 0.07	0.36 0.29	0.00 0.00	0.00 0.00	0.00 0.00	0.00 0.00	0.00 0.00	0.00 0.00
	0.07 0.14	0.07 0.07	0.07 0.14	0.14 0.00	0.00 0.00	0.00 0.00	0.07 0.07	0.00 0.00	0.00 0.00	0.00 0.00	0.00 0.00	0.00 0.00	0.00 0.00
	0.14 0.07	0.07 0.14	0.07 0.07	0.14 0.07	0.21 0.21	0.14 0.21	0.21 0.21	0.21 0.21	0.21 0.21	0.21 0.21	0.21 0.21	0.21 0.21	0.21 0.21
	0.07 0.00	0.07 0.07	0.07 0.07	0.07 0.07	0.00 0.00	0.07 0.07	0.07 0.14	0.07 0.00	0.07 0.00	0.07 0.00	0.07 0.00	0.07 0.00	0.07 0.00
	0.07 0.07	0.07 0.07	0.14 0.14	0.07 0.14	0.00 0.00	0.00 0.00	0.00 0.00	0.00 0.00	0.00 0.00	0.00 0.00	0.00 0.00	0.00 0.00	0.00 0.00
Label	0.36 0.36	—	—	—	—	0.07 0.07	—	—	—	—	—	—	—
	0.14 0.07	—	—	—	—	0.00 0.00	—	—	—	—	—	—	—
	0.57 0.00	—	—	—	—	0.21 0.50	—	—	—	—	—	—	—
	0.07 0.07	—	—	—	—	0.00 0.14	—	—	—	—	—	—	—
	0.00 0.00	—	—	—	—	0.00 0.00	—	—	—	—	—	—	—
KL	0.00 0.36	0.00 0.14	0.14 0.14	0.29 0.21	0.00 0.00	0.00 0.00	0.00 0.00	0.00 0.00	0.00 0.00	0.00 0.00	0.00 0.00	0.00 0.00	0.00 0.00
	0.00 0.07	0.00 0.07	0.07 0.07	0.29 0.21	0.00 0.00	0.00 0.00	0.00 0.00	0.00 0.00	0.00 0.00	0.00 0.00	0.00 0.00	0.00 0.00	0.00 0.00
	0.14 0.29	0.29 0.07	0.07 0.29	0.43 0.43	0.29 0.21	0.43 0.21	0.43 0.36	0.29 0.21	0.43 0.36	0.29 0.21	0.43 0.36	0.29 0.21	0.43 0.36
	0.07 0.07	0.14 0.14	0.07 0.21	0.29 0.36	0.00 0.07	0.00 0.14	0.07 0.14	0.07 0.07	0.07 0.14	0.07 0.07	0.07 0.07	0.07 0.07	0.07 0.07
	0.07 0.00	0.07 0.00	0.43 0.36	0.07 0.29	0.00 0.00	0.00 0.00	0.00 0.00	0.00 0.00	0.00 0.00	0.00 0.00	0.00 0.00	0.00 0.00	0.00 0.00
CE	0.07 0.36	0.07 0.14	0.14 0.21	0.14 0.93	0.00 0.00	0.00 0.00	0.00 0.00	0.00 0.00	0.00 0.00	0.00 0.00	0.00 0.00	0.00 0.00	0.00 0.00
	0.14 0.14	0.00 0.07	0.00 0.07	0.14 0.86	0.00 0.00	0.00 0.00	0.00 0.00	0.00 0.00	0.00 0.00	0.00 0.00	0.00 0.00	0.00 0.00	0.00 0.00
	0.36 0.36	0.36 0.14	0.07 0.21	0.36 0.29	0.29 0.43	0.57 0.36	0.36 0.36	0.36 0.36	0.36 0.36	0.36 0.36	0.36 0.36	0.36 0.36	0.36 0.36
	0.07 0.07	0.14 0.14	0.21 0.29	0.14 0.21	0.07 0.14	0.07 0.14	0.00 0.14	0.29 0.07	0.00 0.00	0.00 0.00	0.00 0.00	0.00 0.00	0.00 0.00
	0.07 0.00	0.07 0.00	0.36 0.29	0.07 0.29	0.00 0.00	0.00 0.00	0.00 0.00	0.00 0.00	0.00 0.00	0.00 0.00	0.00 0.00	0.00 0.00	0.00 0.00
Poisoned Model Detection on Imagenette													
Distance Metrics and Distance Test Sets													
	train	test	rand	inv	adv	train	test	rand	inv	adv	train	test	rand
Cos	0.79 0.93	0.36 0.50	0.29 0.07	0.00 1.00	0.29 0.29	0.29 0.29	0.07 0.93	0.07 1.00	0.00 0.00	0.00 0.00	0.00 0.00	0.00 0.00	0.00 0.00
	0.36 0.36	0.21 0.43	0.07 0.36	0.00 1.00	0.07 0.21	0.21 0.36	0.21 0.36	0.50 0.64	0.00 0.00	0.00 0.00	0.00 0.00	0.00 0.00	0.00 0.00
	0.29 0.71	0.36 0.36	0.21 0.71	0.29 0.71	0.57 0.64	0.57 0.57	0.57 0.43	0.57 0.64	0.00 0.00	0.00 0.00	0.00 0.00	0.00 0.00	0.00 0.00
	0.29 0.43	0.14 0.07	0.21 0.14	0.43 0.43	0.00 0.21	0.29 0.21	0.14 0.14	0.14 0.36	0.00 0.00	0.00 0.00	0.00 0.00	0.00 0.00	0.00 0.00
	0.00 0.14	0.00 0.14	0.00 0.00	0.00 0.79	0.00 0.07	0.00 0.00	0.07 0.14	0.21 0.14	0.00 0.00	0.00 0.00	0.00 0.00	0.00 0.00	0.00 0.00
CosL	0.36 0.57	0.21 0.07	0.57 0.29	0.36 0.57	0.07 0.00	0.21 0.14	0.43 0.14	0.14 0.07	0.00 0.00	0.00 0.00	0.00 0.00	0.00 0.00	0.00 0.00
	0.14 0.29	0.07 0.07	0.21 0.21	0.36 0.21	0.00 0.00	0.00 0.00	0.14 0.14	0.07 0.07	0.00 0.00	0.00 0.00	0.00 0.00	0.00 0.00	0.00 0.00
	0.21 0.14	0.36 0.14	0.14 0.07	0.21 0.14	0.21 0.64	0.29 0.43	0.29 0.64	0.21 0.64	0.00 0.00	0.00 0.00	0.00 0.00	0.00 0.00	0.00 0.00
	0.21 0.07	0.14 0.07	0.21 0.07	0.21 0.14	0.07 0.07	0.07 0.07	0.07 0.07	0.07 0.00	0.00 0.00	0.00 0.00	0.00 0.00	0.00 0.00	0.00 0.00
	0.07 0.21	0.14 0.14	0.07 0.21	0.29 0.21	0.00 0.00	0.00 0.00	0.00 0.00	0.00 0.00	0.00 0.00	0.00 0.00	0.00 0.00	0.00 0.00	0.00 0.00
Label	0.57 0.93	—	—	—	—	0.29 0.36	—	—	—	—	—	—	—
	0.64 0.71	—	—	—	—	0.14 0.29	—	—	—	—	—	—	—
	0.07 0.64	—	—	—	—	0.21 0.71	—	—	—	—	—	—	—
	0.14 0.50	—	—	—	—	0.14 0.14	—	—	—	—	—	—	—
	0.00 0.14	—	—	—	—	0.00 0.00	—	—	—	—	—	—	—
KL	0.36 0.93	0.29 0.29	0.36 0.29	1.00 1.00	0.14 0.36	0.43 0.21	0.43 0.29	0.36 0.29	0.00 0.00	0.00 0.00	0.00 0.00	0.00 0.00	0.00 0.00
	0.21 0.36	0.07 0.00	0.21 0.43	0.00 0.93	0.07 0.07	0.07 0.00	0.07 0.00	0.29 0.29	0.00 0.00	0.00 0.00	0.00 0.00	0.00 0.00	0.00 0.00
	0.43 0.71	0.07 0.50	0.57 0.64	0.36 0.71	0.29 0.57	0.14 0.71	0.21 0.71	0.29 0.57	0.00 0.00	0.00 0.00	0.00 0.00	0.00 0.00	0.00 0.00
	0.21 0.21	0.14 0.29	0.29 0.29	0.21 0.50	0.07 0.07	0.00 0.07	0.07 0.07	0.07 0.07	0.00 0.00	0.00 0.00	0.00 0.00	0.00 0.00	0.00 0.00
	0.29 0.57	0.21 0.57	0.57 0.93	0.50 0.50	0.07 0.07	0.07 0.14	0.21 0.07	0.00 0.21	0.00 0.00	0.00 0.00	0.00 0.00	0.00 0.00	0.00 0.00
CE	0.07 0.93	0.29 0.64	0.36 0.21	1.00 1.00	0.14 0.21	0.43 0.21	0.43 0.00	0.50 0.29	0.00 0.00	0.00 0.00	0.00 0.00	0.00 0.00	0.00 0.00
	0.14 0.57	0.21 0.29	0.21 0.43	0.00 0.93	0.00 0.07	0.00 0.00	0.14 0.07	0.36 0.21	0.00 0.00	0.00 0.00	0.00 0.00	0.00 0.00	0.00 0.00
	0.36 0.57	0.29 0.71	0.07 0.50	0.29 0.57	0.00 0.64	0.07 0.71	0.07 0.71	0.07 0.71	0.00 0.00	0.00 0.00	0.00 0.00	0.00 0.00	0.00 0.00
	0.29 0.07	0.07 0.29	0.43 0.29	0.29 0.50	0.14 0.14	0.00 0.07	0.00 0.07	0.00 0.07	0.00 0.00	0.00 0.00	0.00 0.00	0.00 0.00	0.00 0.00
	0.29 0.64	0.21 0.57	0.64 0.93	0.50 0.50	0.00 0.07	0.14 0.14	0.07 0.14	0.07 0.21	0.00 0.00	0.00 0.00	0.00 0.00	0.00 0.00	0.00 0.00
Poisoned Model Detection on Imagenette													
	train	test	rand	inv	adv	train	test	rand	inv	adv	train	test	rand

Figure 7: FPR and FNR under all the combinations of the components of our framework: distance test sets, sample-wise distances, aggregations, and model pools.

Table 3: Youden’s J statistic on CIFAR-10 model pools of different robustness. The best J values in each column are in bold.

	standard	$\epsilon = 4/255$	$\epsilon = 8/255$
Inverted	0.86	0.86	0.86
Adversarial	0.86	1.00	1.00
Test	0.86	1.00	1.00
Train	0.79	0.86	0.93
Random	0.79	0.64	0.64
ModelDiff [45]	0.79	1.00	0.86
K-ARM [28]	0.36	0.00	-0.07
DFTND [31]	0.00	0.00	0.00
SCALE-UP [32] Inverted	0.43	0.21	0.21
SCALE-UP [32] Test	0.21	0.21	0.14
SCALE-UP [32] Training	0.14	0.29	0.07
SODA [37]	0.07	0.14	0.64

Table 4: Youden’s J statistic on Imagenette model pools of different robustness. The best J values in each column are in bold.

	standard	$\epsilon = 4/255$	$\epsilon = 8/255$
Inverted	0.79	0.86	0.86
Adversarial	0.71	1.00	0.86
Test	0.86	1.00	0.86
Training	0.71	0.64	0.71
Random	0.50	0.29	0.43
ModelDiff [45]	0.29	0.79	0.64
K-ARM [28]	0.00	0.00	0.00
Ex-Ray [36] Test	0.21	0.07	0.00
Ex-Ray [36] Training	0.07	0.21	0.21
SCALE-UP [32] Inverted	0.50	0.21	0.14
SCALE-UP [32] Test	0.36	0.14	0.29
SCALE-UP [32] Training	0.50	0.14	0.36

consistent preference for either false positives or false negatives, which is expected due to Youden’s J treating them equally (after normalization). In principle, this metric can be swapped out in favor of another in the threshold calibration process (see Section 5.1.2) to match the authority’s preferences.

The main conclusions we can draw from these results are the following.

- After considering both tasks, CosL is the most reliable choice for sample-wise distance
- Robust model pools perform better overall, indicating that the authority should use robust training tasks to test the provider
- As for distance test sets, the random set and the training set are both inferior, and the best choice is either the test set or the adversarial set
- Regarding aggregation, the standard deviation is a robust choice overall.

Based on these results, in the following we will assume CosL as sample-wise distance and standard deviation as aggregation, if not otherwise stated.

Fixing these choices, we compare our method with other approaches in Tables 3 and 4. This time, all the three robustness levels described previously are included for both tasks.

DFTND [31] classified each CIFAR-10 model as clean. The largest detection score was 14.22, which is significantly below their threshold of 100. The K-Arm backdoor detector [28] is designed to look for small triggers. It probably fails in this application because semantic backdoors do not have any such triggers. SCALE-UP [32] and SODA [37] show a reasonably good performance in some scenarios. Still, our approach is significantly better.

ModelDiff [45] is reasonably good, but it is outperformed by our best settings as well, especially on Imagenette.

Table 5: Statistics on CIFAR-10 model pools of various model architectures. The best J values in each column are in bold.

Metric	WR28-10	ConvNeXt	ViT
Accuracy	0.96	0.9	0.82
ASR	0.92	0.84	0.78
J (Inverted)	0.57	0.21	0.86
J (Adversarial)	1.00	0.86	1.00
J (Test)	1.00	0.86	1.00
J (Training)	0.71	0.93	1.00
J (Random)	0.36	0.36	0.36

6.4 Additional Architectures

Although in our application scenario the authority is free to select the model architecture, we test architectures other than ResNet-18. In more detail, for the CIFAR-10 dataset, we tested WideResNet-28-10 [60], ConvNeXt V2 [61], and the vision transformer ViT [62].

Our model pools for all the three architectures consisted of 14 clean and 14 poisoned models. These pools are not robust. For WideResNet, the same hyperparameters were used for training as in the case of the ResNet-18 pool. The ConvNeXt V2 model used the following setup: depths=2,2,2,2 dims=40,80,160,320 kernel=3 stem=1 drop=0.0 scale=0. For the ViT model we used the small version with the parameters patch=4, dim=192, depth=12, heads=3, mlp=768. The training used 400 epochs with a batch size of 256. We used the AdamW [63] optimizer with a learning rate of 10^{-3} for the last two model types.

Youden’s J statistics (with CosL distance and standard deviation aggregation) are presented in Table 5. For each pool, we also present the average accuracy of all the models, and the average ASR of the poisoned models.

As before, the test and adversarial distance test sets perform best, giving a perfect performance of J=1 for WideResNet and ViT. In general, the method is robust to the choice of architecture, and it is also remarkable that the best performance is given by the transformer architecture ViT, a popular choice today.

6.5 Additional Datasets

The authority is also free to choose the dataset to use when mystery shopping. In this section, we evaluate additional datasets beyond CIFAR-10 and Imagenette, namely Imagewoof [54] and VGGFaces2 [64].

Imagewoof is a subset of ImageNet that includes various dog breeds. We trained a ResNet-18 model pool on the Imagewoof dataset using the same parameters as previously described for Imagenette.

VGGFaces2 is a dataset designed for face recognition tasks. Its training set contains 8,631 identities. For our experiments, we randomly selected 100 identities from those with at least 400 images each, creating a 100-class face classification task. We constructed the validation and test sets using 10% of the original training examples for both sets. To perform a semantic backdoor attack, we selected a random class from the original VGGFaces2 test set. Backdoor classes were also assigned 10% validation and test splits.

It is important to note that the original VGGFace2 training and test sets contain disjoint identities, ensuring no overlap between them. The same training hyperparameters used for Imagenette were applied here as well.

These pools are not robust.

We present the results in Table 6, where we include the results for CIFAR-10 and Imagenette (see Tables 3 and 4) for comparison. For each dataset, we can find settings where our method provides a good performance, so we can conclude that the method is robust to datasets as well, given that the authority can select the distance test set freely for a given dataset. It is interesting, though, that for the VGGFaces2 dataset, the inverted distance test set performed very poorly, while the training set performed best. An explanation could be that our pools here are not robust; but this observation needs further study.

6.6 Multi-class Backdoor Attack

In most of our experiments, each model contained at most one backdoor, since we hypothesized that this is the most challenging scenario for our method. To confirm this, we also trained standard and robust CIFAR-10 poisoned models

Table 6: Statistics on ResNet-18 model pools with various datasets. The best J values in each column are in bold.

Metric	CIFAR-10	Imagenette	Imagewoof	VGGFace2
Accuracy	0.94	0.90	0.78	0.96
ASR	0.90	0.90	0.94	0.96
J (Inverted)	0.86	0.79	0.57	0.07
J (Adversarial)	0.86	0.71	0.79	0.36
J (Test)	0.86	0.86	0.43	0.50
J (Training)	0.79	0.71	0.29	0.71
J (Random)	0.79	0.50	0.07	-0.43

Table 7: Youden’s J statistic on CIFAR-10 model pools with multi-class attacks. The best J values in each column are in bold.

	standard	$\epsilon = 8/255$
Inverted	1.00	1.00
Adversarial	1.00	1.00
Test	1.00	1.00
Train	1.00	1.00
Random	0.79	0.86
SODA [37]	0.14	0.21

where all ten classes are attacked at the same time. (The set of clean models remained the same as before.) The poisoning was based on the method described in Section 6.1.1, with the additional requirement that a model cannot use the same OOD class for multiple target classes. The average accuracy was 0.93 and 0.80 for the standard and robust poisoned models, respectively, and the average ASR was 0.86 and 0.70.

The results are shown in Table 7. We can see that this scenario is indeed easy for our method. However, it is detrimental to SODA, as it relies on finding outliers over the classes.

6.7 Statistical Analysis

Since the evaluation of detection performance is based on relatively few samples, it is worthwhile to make sure that our findings are statistically significant. Until this point, the experiments used cross-validation over 14 clean and 14 poisoned models, meaning J values were calculated based on 28 samples. We can use the one-tailed binomial test to calculate the p -value: how likely that an observed ratio of correctly classified samples ($(J + 1)/2$ in the balanced case) can be achieved by random guessing. If the p -value is less than a given threshold, we can reject the null hypothesis that our method is not better than random guessing.

Table 8 lists the possible non-negative J values (along with the corresponding sum of the true positive and true negative samples) and the calculated p -values. Using 0.05 as the threshold for the p -value, we can conclude that J values above 0.3 (which was surpassed in the experiments detailed in the previous sections) are statistically significant for these pools. The table also includes the infimum of the 95% confidence interval for J . (Note that the supremum is 1 due to the test being one-tailed.)

6.8 The Size of the Model Pool

We created a larger model pool to examine the effect of model pool size. That is, we created 36 additional clean and 36 additional poisoned models to extend the previously used Imagenette robust model pool ($\epsilon_\infty = 4/255$). This gave us 50 clean and 50 poisoned models.

From this pool, we randomly selected 10 clean and 10 poisoned models to form a test set. Instead of cross-validation, here we opted for a separate test set in order to be able to evaluate the pools of different sizes on the exact same test set.

To estimate the expected performance of the authority having m clean and m poisoned models in its own pool, we sampled 500 random pools of size $m + m$ for every setting of m . For each sampled pool of size $m + m$, we used our method to make predictions for each model in the test set, and calculated Youden’s J. Then we averaged J over the 500 training pools.

Table 8: Correspondence between the number of correctly classified samples, Youden’s J statistic, and p-value, assuming a balanced set of 28 samples and using random guessing as the null hypothesis. Also shown is the infimum of the 95% confidence interval for J.

TP+TN	J	P-value	95% CI
14	0.00	0.574722990	-0.33
15	0.07	0.425277010	-0.27
16	0.14	0.285794094	-0.20
17	0.21	0.172464225	-0.13
18	0.29	0.092466671	-0.06
19	0.36	0.043579277	0.01
20	0.43	0.017849069	0.09
21	0.50	0.006270476	0.16
22	0.57	0.001859583	0.24
23	0.64	0.000456117	0.32
24	0.71	0.000089996	0.40
25	0.79	0.000013720	0.49
26	0.86	0.000001516	0.58
27	0.93	0.000000108	0.68
28	1.00	0.000000004	0.80

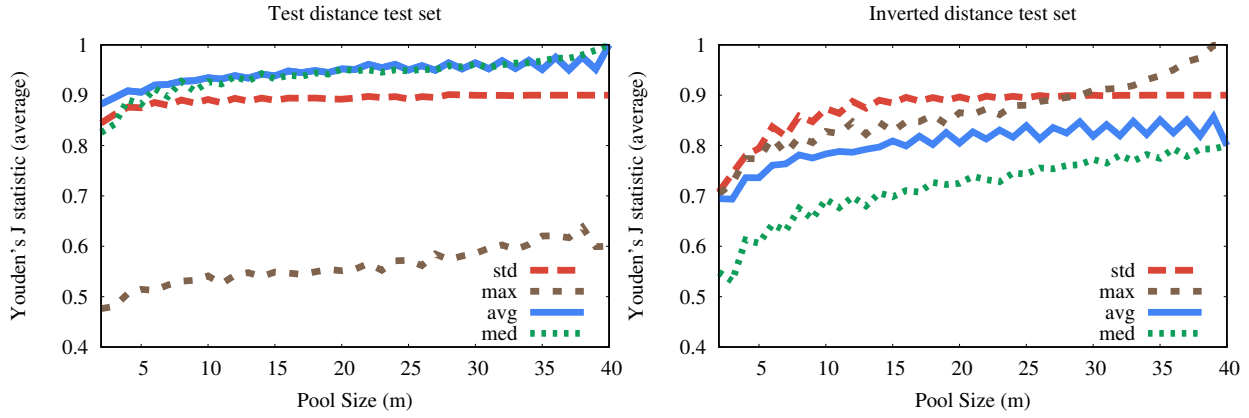


Figure 8: Performance as a function of the pool size of the authority, for two distance test sets (Test (left) and Inverted (right)) and different aggregations.

The results for $2 \leq m \leq 40$ are shown in Fig. 8, using test and inverted images as distance test sets. Note that there is only one possible training set when $m = 40$, and due to this, and the size of the test set, J is a multiple of 0.1 in this case.

Increasing m does not result in a significant gain in the best performance except when m is small.

6.9 Detecting an Adaptive Attack

Although the provider can always decide not to insert a backdoor if it suspects that a mystery shopping is taking place, it is necessary to consider the possibility that the provider is aware of the detection method that the authority might use and it actively tries to avoid the detection of the inserted backdoor.

Here, we assume that the provider knows the exact method that will be used for detection. The goal of the provider is to poison the model in such a way that our detection method fails. This can best be achieved if the sample-wise distance function we apply does not differentiate between poisoned and clean models.

Let the sample-wise distance be CosL, the best performing choice so far. We propose an adaptive attack against this distance function based on the idea of distillation [65], a known approach for hiding backdoors [66]. First, the provider

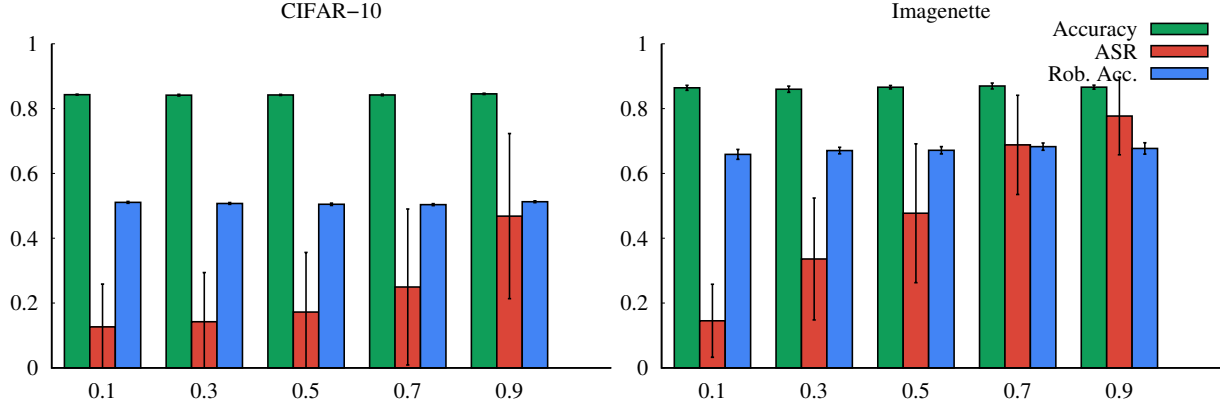


Figure 9: Basic model statistics (accuracy, attack success rate (ASR), and robust accuracy) on the robust CIFAR-10 (left) and robust Imagenette (right) adaptive model pools for different values of the α parameter.

trains a clean model θ^* , and then it trains a poisoned model $\tilde{\theta}$ using a loss function that combines an accuracy objective and a distillation objective that acts on the logit layer.

Let $D_p = D \cup B$ be the poisoned dataset with B containing the backdoor samples. The loss function of a sample $(x, y) \in D_p$ on model θ is

$$\ell((x, y), \theta) = \alpha \text{CrossEntropy}(f(x, \theta), y) + \mathbb{1}_D(x, y)(1 - \alpha) \text{CosL}(z(x, \theta^*), z(x, \theta)), \quad (9)$$

where the second term is the distillation term minimizing sample-wise distance. Parameter $\alpha \in [0, 1]$ represents the tradeoff between cross-entropy and distillation. The indicator function $\mathbb{1}_D$ makes sure that only clean training samples use distillation.

During this adaptive attack, the adversary initializes the model with the weights of its clean reference model.

6.9.1 New model pools

To evaluate the adaptive poisoning attack, we created new model pools of 14 clean and 14 poisoned models. More precisely, we created a new Imagenette robust ($\epsilon_\infty = 4/255$) model pool and a CIFAR-10 robust ($\epsilon_\infty = 8/255$) model pool for every $\alpha \in \{0.1, 0.3, 0.5, 0.7, 0.9\}$. The pools with different values of α share the same 14 clean models with each other and their corresponding non-adaptive pool. Figure 9 depicts the basic properties of these pools.

6.9.2 Evaluation of adaptive pools

Let us first examine the J statistics obtained with the combinations of our distance test sets and aggregation types, following the same methodology as used in Section 6.3. Figure 10 shows the results got just using the models with $0.25 \leq \text{ASR}$. The inverted distance test set combined with the standard deviation aggregation method is the most stable option.

Figure 11 shows the same data in a plot format, but with only the standard deviation aggregation, and adding the case of unfiltered model pools ($0 \leq \text{ASR}$) and pools with $0.5 \leq \text{ASR}$. Here, with low values of α , where the backdoor behavior is most hidden, the inverted distance test set clearly outperforms the other alternatives for all the thresholds of ASR. Also, for higher ASR thresholds the inverted set performs best overall. Recall that models with a high ASR are interesting because these models are those where the adaptive attack was the most successful.

6.9.3 Ablations of Inverse Image Generation

Now that we have established that the inverted distance test set is the most promising approach in the harder cases, let us perform an ablation study of this set generation method. We do this by evaluating a number of variants of the method, namely

- *Without a prior*: we optimize the input image directly without using a prior generator network

CIFAR-10, $0.25 \leq \text{ASR}$				Imagenette, $0.25 \leq \text{ASR}$						
Alpha Values and Distance Test Sets	$\alpha = 0.9$	test	-0.07	0.10	0.55	-0.07	-1.00	0.43	0.29	-1.00
		inv	0.58	0.66	0.66	-0.41	0.86	1.00	1.00	0.36
		adv	0.77	0.91	0.68	0.93	0.00	0.86	0.86	-0.07
	$\alpha = 0.7$	test	-0.14	0.11	0.44	-0.71	-1.00	0.21	0.07	-1.00
		inv	0.31	0.60	0.40	0.66	0.57	0.93	0.86	0.21
		adv	1.00	0.86	0.33	1.00	0.00	0.71	0.64	-0.07
	$\alpha = 0.5$	test	-0.07	-0.14	0.25	-0.07	-0.14	-0.02	0.07	-0.14
		inv	0.68	0.46	0.29	0.68	0.49	0.66	0.42	-0.12
		adv	0.68	0.36	0.04	0.68	-0.93	0.75	0.28	-0.09
	$\alpha = 0.3$	test	-0.07	-0.36	0.17	-0.07	-0.14	0.07	0.14	-0.14
		inv	0.67	0.60	0.60	1.00	0.56	0.56	0.13	0.71
		adv	0.05	-0.14	-0.19	0.60	-0.29	0.39	0.31	-0.11
	$\alpha = 0.1$	test	-0.07	-0.07	0.36	-0.07	-0.29	0.36	0.21	-0.14
		inv	1.00	0.60	0.60	1.00	0.43	0.29	0.07	0.43
		adv	-0.07	-0.14	-0.64	-0.07	-0.43	0.43	0.29	-0.29
Aggregation Types				Aggregation Types						
avg	std	max	med	avg	std	max	med			

Figure 10: Youden’s J statistic with the CosL distance and the adaptive model pools for different α values, distance test sets, and aggregations.

- *Single step*: instead of the two-step method, we solve the problem in Eq. (7) by directly optimizing the prior generator network in a single step
- *Invert only*: we simply invert the network using the prior generator network, but we perform no other optimization

Figure 12 shows our results with the ablated versions of inverted distance test set generation. Across almost all α values, the proposed method outperformed the simplified variants, confirming that all the design elements contribute to the effectiveness of our approach.

6.10 A Diverse Model Pool

Here, we evaluate the realistic case where the provider takes advantage of the degrees of freedom available to it to create different kinds of backdoors. To model this, we create a test model pool (to model the provider) that contains a diverse set of models, and we create a larger training model pool (the pool of the authority) that also captures the diverse training strategies we examined. Note that in our application scenario *the authority controls the recipe of training*, and the provider gains nothing by deviating from this, as such deviations only increase the chance of detection. Therefore, the degree of freedom available to the provider (apart from selecting the backdoor distribution) is whether it applies an adaptive attack strategy.

We evaluate this scenario on Imagenette, using robust ($\epsilon_\infty = 4/255$) training. Recall that the authority controls the type of training and the dataset as well, so this choice does not cause any loss of generality. We start with the pool used in Section 6.8 which contains 50 clean and 50 poisoned models. We include 40 clean and 40 poisoned randomly selected models in the training pool and the remaining models are inserted into the test pool.

We extended the set of models using all the adaptive attack model pools we evaluated in Section 6.9. To be more precise, we included 50 adaptively poisoned models from these pools (selected from the models with $0.25 \leq \text{ASR}$) in the training pool. We trained 50 additional clean models and added these to the training pool as well. Altogether, the training pool contained 90 poisoned models of several types and 90 clean models.

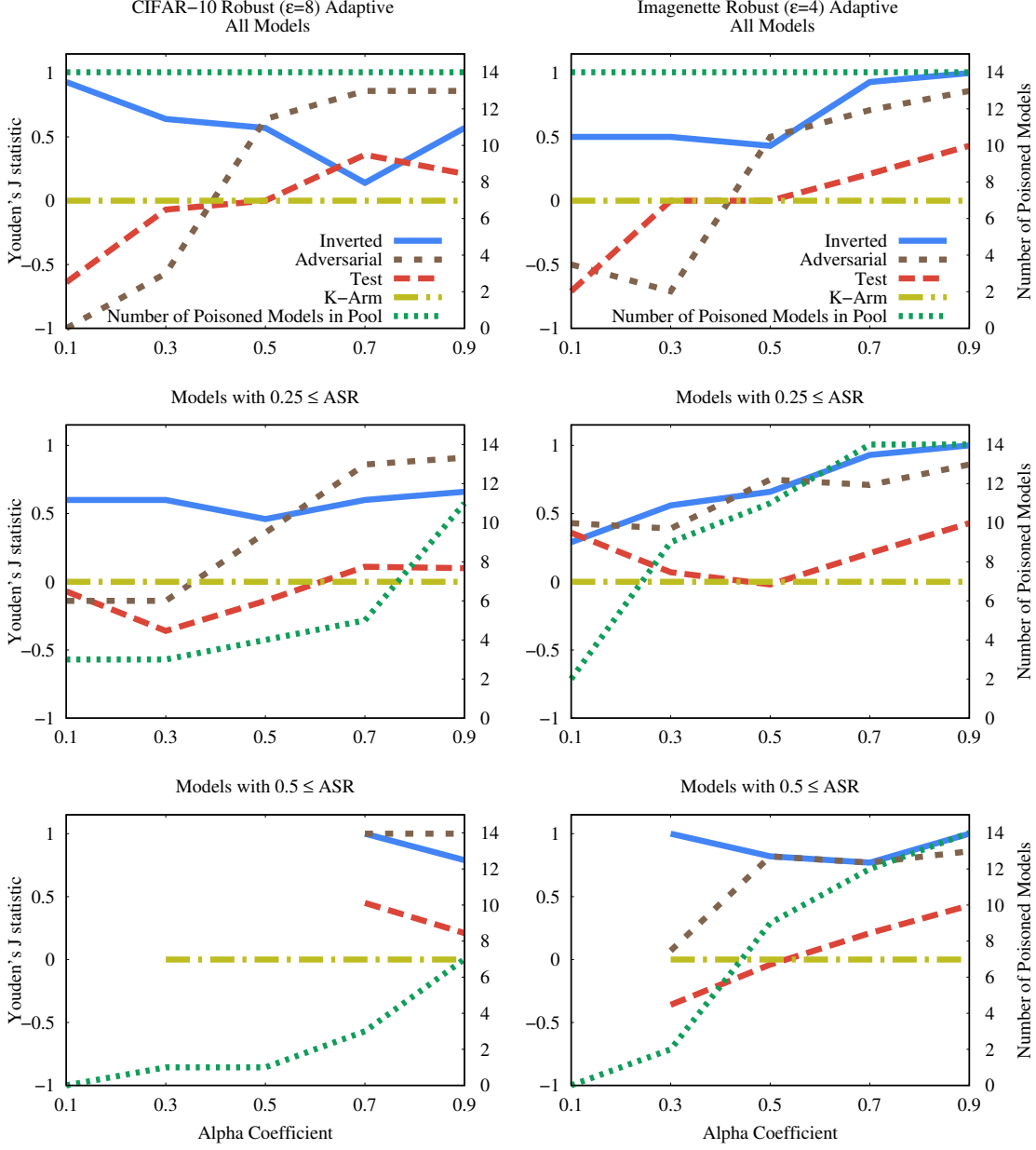


Figure 11: Youden’s J statistic for detecting the adaptive attack as a function of the α coefficient. The CosL distance and standard deviation aggregation were used. The number of poisoned models is indicated on the right vertical axis. Note that if the number of poisoned models is fewer than two then the evaluation of our method is not well-defined.

We also extended the test pool by training 5 adaptively poisoned models for every $\alpha \in \{0.5, 0.7, 0.9\}$, hence we added 15 models in total. We also trained 15 new clean models and added these to the test pool. Note that these models all have $0.25 \leq \text{ASR}$. This way, the test pool contained 25 poisoned and 25 clean models.

We now present the results in Table 9. In the first column, a small pool of size 28 was sampled from the large pool of 180 models independently (but with an equal number of clean and poisoned models) 500 times, and the average of the resulting 500 J values is included in the table. In the second column, the full pool was used. In both cases, the test pool was used for evaluation.

The best J that we got was with our method using the Inverted distance test set.

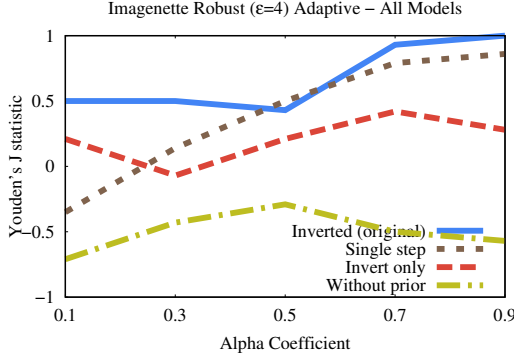


Figure 12: Ablations of Inverted distance test set generation.

Table 9: Youden’s J statistic on the diverse pool. The best J values in each column are in bold.

Size of training model pool:	28	180
Inverted	0.68	0.72
Test	0.39	0.48
ULP [34]	-	0.28
K-ARM [28]	0.00	0.00
Ex-Ray [36] (test data)	-0.04	-0.04
Ex-Ray [36] (train data)	0.08	0.08

The large training pool allows us to test ULP [34], which is based on training a meta-classifier over the models in the training pool and so requires a large model pool.

We used the hyperparameters suggested by the authors. Out of fairness, we should mention that ULP is based on the assumption that the training backdoor models contain the same trigger pattern as the test models, which is not the case in our scenario.

We also include results obtained with Ex-Ray [36] and K-Arm [28], but we should add that these methods do not use training at all, so the results shown here were simply calculated based on the test model pool.

6.11 Generalization over Attack Types

The provider has a limited degree of freedom because it must create models that appear very similar to those that are requested by the authority. Still, the adaptive attack represents a possible source of variability, because we can set different values of α . Here, we discuss how robust the detection method is to this source of variability. We do this by evaluating all the possible cases where the authority and the provider use different attack methods.

Figure 13 shows the J statistics with all such combinations. We measure J with the help of the adaptive attack model pools described earlier. In more detail, the optimal decision threshold is calculated using the authority’s model pool (the training pool) and J is calculated based on the classification of the models in the provider’s pool (the test pool) using this threshold.

The method is robust, as there are only a few cases where J is small. Most importantly, the *non-adaptive (vanilla) training pool is robust* when using the inverted distance test set and standard deviation aggregation.

6.12 The Inverted Distance Test Set: Examples

Motivated by the performance of the inverted distance test set, let us take a closer look at examples of such sets on CIFAR-10. Figure 14 shows two sets of generated inputs: one generated based on a clean model, and one based on a poisoned model. The poisoned class was the ‘horse’ class, and the backdoor OOD distribution was chosen to be the ‘fruits and vegetables’ superclass of CIFAR-100.

This example demonstrates the intuition behind model inversion: our inversion algorithm is biased towards *realistic input samples that are different from clean samples*, so it creates fruit-like images that activate the ‘horse’ class. These

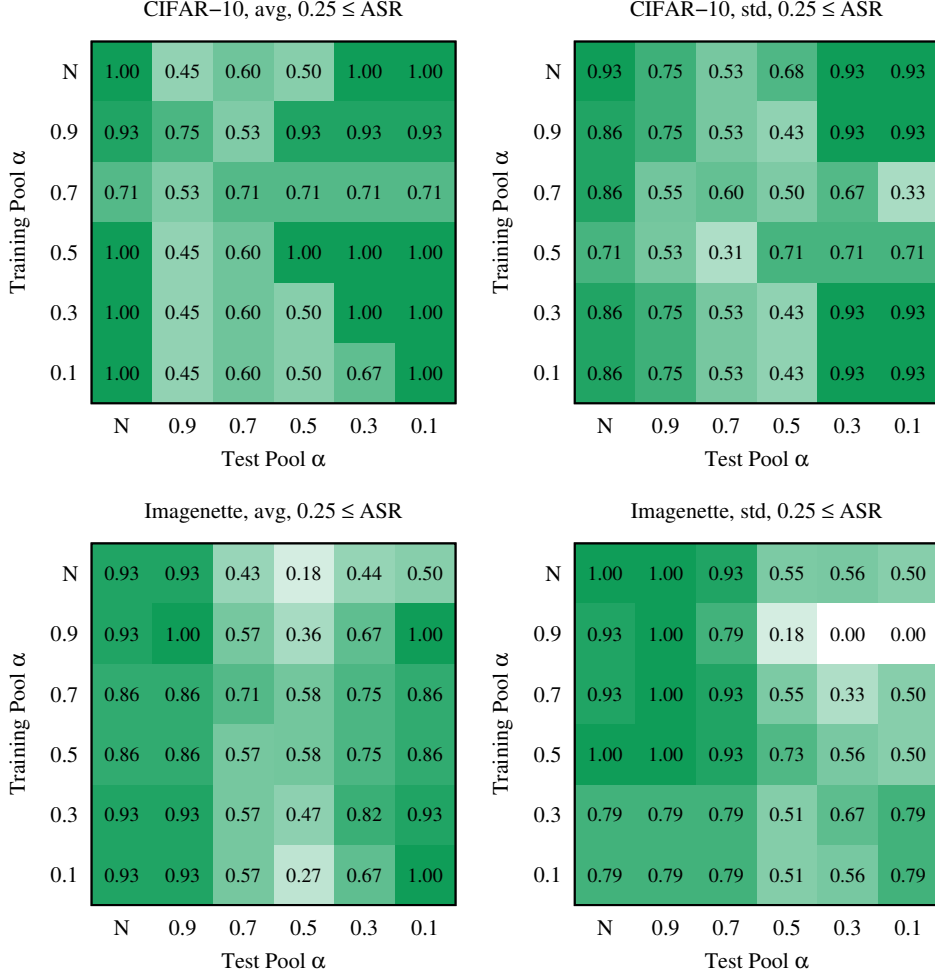


Figure 13: Youden’s J statistic for all possible combinations of attacks methods used by the authority (vertical axis) and the provider (horizontal axis). In each case, the CosL distance was used on the inverted distance test set. Two aggregation methods are included, namely average and standard deviation. ‘N’ denotes the non-adaptive robust pool.

generated backdoor inputs are very far from clean images. This in turn results in a large sample-wise distance between the clean and poisoned models over such generated inputs.

Figure 15 shows the effect of the adaptive attack. Recall that for small α values the adaptive attack is weaker and the backdoors are harder to activate. Indeed, for $\alpha = 0.1$ the generated images are less fruit-like.

7 Conclusions

We studied a mystery shopping scenario where a consumer protection authority tests whether a MLaaS provider inserts semantic backdoors during a training task. In our method, the authority creates a small model pool containing clean and poisoned models and calibrates a decision method based on this pool.

We showed through a large set of experiments that among the many options we examined, the most robust one across the board is based on using adversarial training as a mystery shopping task, and model distance is best measured using the CosL distance (the cosine distance of the logit layers) over a set of samples that are generated using model-inversion, biased towards generating backdoor inputs for poisoned classes. This method shows good performance even in detecting adaptive attacks by the provider.

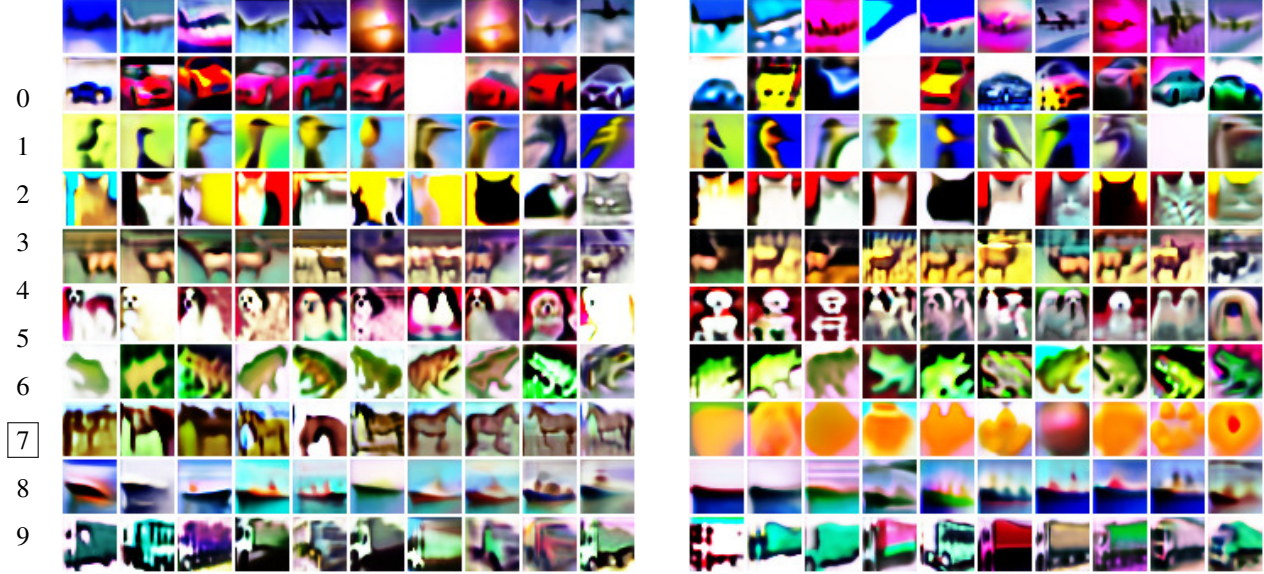


Figure 14: CIFAR-10 Inverted distance test set images for a clean robust model ($\epsilon = 8/255$, left) and for a poisoned robust model ($\epsilon = 8/255$, right)). Poisoned class: horse (7), backdoor class: fruit and vegetables (CIFAR-100-4). CIFAR-10 classes are listed top down, starting from class 0.

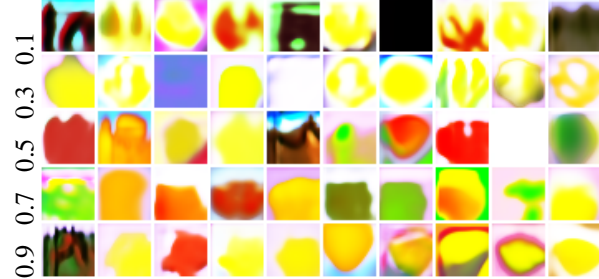


Figure 15: CIFAR-10 inverted images for robust models ($\epsilon = 8/255$) with different values of α (adaptive attack parameter). Poisoned class: horse (7), backdoor class: fruit and vegetables (CIFAR-100-4). Only the poisoned class is shown.

7.1 Practical Considerations

Here, we share some thoughts on a number of practical issues related to our research from the point of view of consumer protection authorities. These include the cost of the methodology and some ethical and legal considerations.

7.1.1 Cost

Our method involves training model pools on a given problem, and our best pools are based on adversarial training. Due to these factors, the cost will be about two orders of magnitude higher than that of training a single model. Also, the authority needs to have access to expert knowledge in order to design and create the pools.

On the other hand, this investment has to be made only once and the resulting detection thresholds will remain usable any number of times for mystery shopping, as long as the testing task remains a secret.

7.1.2 Legal and Ethical Issues

Our results do not open any new legal or ethical issues within machine learning, in fact, our scenario is less problematic than usual because *the trained models are not actually deployed*. They remain private and unused. However, the idea of using mystery shopping in this context is somewhat unusual so it is worth considering some of the implications.

Since mystery shopping will most likely be executed by sub-contractors to hide the identity of the authority, it is imperative that these sub-contractors are aware of the nature of the task they are carrying out. Also, it is advisable to publicly announce that the given authority executes such mystery shopping projects for quality control and as a safety measure.

Obviously, the data involved in the project must comply with every data protection regulation applicable to the given authority, despite the fact that the trained models are never deployed.

7.2 Limitations

Let us now mention some of the limitations of our work. Although we assumed that the provider uses a backdoor distribution that is unknown and unpredictable to the authority, the provider can insert extra inputs that might act as backdoors in many ways. In other words, while the attacker is incentivized to include a backdoor that is OOD relative to the clean distribution (otherwise no attack is necessary in the first place), there is an open ended set of possibilities of such OOD distributions that we could obviously not cover experimentally.

Also, evaluating the case of the adaptive attack is essential. We presented a best-effort adaptive attack, but this is also only an empirical argument. The possible set of adaptive attacks is also open-ended and we cannot guarantee that a better attack will not be discovered that is even more successful in hiding the backdoor from our detector.

We should mention here that in some of our experiments we used only two common datasets (CIFAR-10 and Imagenette), and one network architecture (ResNet-18). However, we included tests with additional datasets (VGGFace2 and ImageWoof) and architectures (ConvNeXt and ViT) as well in some scenarios that suggest that the method is robust to these choices. Also, it should be kept in mind that in our scenario the authority controls what dataset and architecture is used. This allows the authority to even optimize the dataset and the architecture to best support the detection method.

Also worth mentioning that our framework is not suitable for testing services that are based on the provider’s private data, as that precludes the authority from creating the necessary reference pool.

While we provide extensive empirical evaluations to demonstrate the effectiveness of our approach, we do not present mathematically rigorous theoretical explanations for our results. The effect of poisoning on model distance is intuitive, but not formally described beyond the metrics themselves.

Furthermore, poisoning is not the only factor that can increase the model distance: for example, a dishonest provider might try to cut costs by training for fewer epochs than agreed upon, or a careless provider might fail to pay attention to the instructions. Our method could easily give a false positive result in these situations. However, similarly to poisoning, such practices negatively impact the customers, therefore their detection is not necessarily a flaw.

Acknowledgments

This work was supported by the European Union project RRF-2.3.1-21-2022-00004 within the framework of the Artificial Intelligence National Laboratory and project TKP2021-NVA-09, implemented with the support provided by the Ministry of Culture and Innovation of Hungary from the National Research, Development and Innovation Fund, financed under the TKP2021-NVA funding scheme.

References

- [1] Christian Szegedy, Wojciech Zaremba, Ilya Sutskever, Joan Bruna, Dumitru Erhan, Ian J. Goodfellow, and Rob Fergus. Intriguing properties of neural networks. In *2nd International Conference on Learning Representations (ICLR)*, 2014. URL <http://arxiv.org/abs/1312.6199>.
- [2] Micah Goldblum, Dimitris Tsipras, Chulin Xie, Xinyun Chen, Avi Schwarzschild, Dawn Song, Aleksander Madry, Bo Li, and Tom Goldstein. Dataset security for machine learning: Data poisoning, backdoor attacks, and defenses. *IEEE Trans. Pattern Anal. Mach. Intell.*, 45(2):1563–1580, 2023. doi: 10.1109/TPAMI.2022.3162397. URL <https://doi.org/10.1109/TPAMI.2022.3162397>.
- [3] Richard Ngo, Lawrence Chan, and Sören Mindermann. The alignment problem from a deep learning perspective. In *The Twelfth International Conference on Learning Representations, ICLR 2024, Vienna, Austria, May 7-11, 2024*. OpenReview.net, 2024. URL <https://openreview.net/forum?id=fh8EYKFKns>.
- [4] Eugene Bagdasaryan, Andreas Veit, Yiqing Hua, Deborah Estrin, and Vitaly Shmatikov. How to backdoor federated learning. In Silvia Chiappa and Roberto Calandra, editors, *Proceedings of the Twenty Third International Conference on Artificial Intelligence and Statistics*, volume 108 of *Proceedings of Machine Learning Research*, pages

2938–2948. PMLR, 26–28 Aug 2020. URL <https://proceedings.mlr.press/v108/bagdasaryan20a.html>.

[5] Tianyu Gu, Kang Liu, Brendan Dolan-Gavitt, and Siddharth Garg. Badnets: Evaluating backdooring attacks on deep neural networks. *IEEE Access*, 7:47230–47244, 2019.

[6] Yingqi Liu, Shiqing Ma, Yousra Aafer, Wen-Chuan Lee, Juan Zhai, Weihang Wang, and Xiangyu Zhang. Trojaning attack on neural networks. In *25th Annual Network And Distributed System Security Symposium (NDSS 2018)*. Internet Soc, 2018.

[7] Aniruddha Saha, Akshayvarun Subramanya, and Hamed Pirsiavash. Hidden trigger backdoor attacks. In *Proceedings of the AAAI conference on artificial intelligence*, volume 34, pages 11957–11965, 2020.

[8] Ali Shafahi, W Ronny Huang, Mahyar Najibi, Octavian Suciu, Christoph Studer, Tudor Dumitras, and Tom Goldstein. Poison frogs! targeted clean-label poisoning attacks on neural networks. *Advances in neural information processing systems*, 31, 2018.

[9] Alexander Turner, Dimitris Tsipras, and Aleksander Madry. Label-consistent backdoor attacks. *arXiv preprint arXiv:1912.02771*, 2019.

[10] Tuan Anh Nguyen and Anh Tran. Input-aware dynamic backdoor attack. *Advances in Neural Information Processing Systems*, 33:3454–3464, 2020.

[11] Ahmed Salem, Rui Wen, Michael Backes, Shiqing Ma, and Yang Zhang. Dynamic backdoor attacks against machine learning models. In *2022 IEEE 7th European Symposium on Security and Privacy (EuroS&P)*, pages 703–718. IEEE, 2022.

[12] Yunfei Liu, Xingjun Ma, James Bailey, and Feng Lu. Reflection backdoor: A natural backdoor attack on deep neural networks. In *Computer Vision–ECCV 2020: 16th European Conference, Glasgow, UK, August 23–28, 2020, Proceedings, Part X 16*, pages 182–199. Springer, 2020.

[13] Ren Pang, Hua Shen, Xinyang Zhang, Shouling Ji, Yevgeniy Vorobeychik, Xiapu Luo, Alex Liu, and Ting Wang. A tale of evil twins: Adversarial inputs versus poisoned models. In *Proceedings of the 2020 ACM SIGSAC conference on computer and communications security*, pages 85–99, 2020.

[14] Emily Wenger, Roma Bhattacharjee, Arjun Nitin Bhagoji, Josephine Passananti, Emilio Andere, Heather Zheng, and Ben Zhao. Finding naturally occurring physical backdoors in image datasets. In S. Koyejo, S. Mohamed, A. Agarwal, D. Belgrave, K. Cho, and A. Oh, editors, *Advances in Neural Information Processing Systems*, volume 35, pages 22103–22116. Curran Associates, Inc., 2022.

[15] Junyu Lin, Lei Xu, Yingqi Liu, and Xiangyu Zhang. Composite backdoor attack for deep neural network by mixing existing benign features. In *Proceedings of the 2020 ACM SIGSAC Conference on Computer and Communications Security, CCS ’20*, pages 113–131, New York, NY, USA, 2020. Association for Computing Machinery. ISBN 9781450370899. doi: 10.1145/3372297.3423362. URL <https://doi.org/10.1145/3372297.3423362>.

[16] Sizheng Wu, Jun Li, Chao Li, Yawei Ren, and Liyan Shen. A universal semantic-based method for backdoor attack. In *9th IEEE International Conference on Data Science in Cyberspace, DSC 2024, Jinan, China, August 23-26, 2024*, pages 414–420. IEEE, 2024. doi: 10.1109/DSC63484.2024.00062. URL <https://doi.org/10.1109/DSC63484.2024.00062>.

[17] Ye Xiao, Wenhan Yao, Zexin Li, Jiangkun Yang, and Weiping Wen. Phoneme semantic backdoor attacks with multiple task learning for speech classification task. In *National Conference on Man-Machine Speech Communication*, pages 79–90. Springer, 2024.

[18] Jiazhai Dai, Zhipeng Xiong, and Chenhong Cao. A semantic backdoor attack against graph convolutional networks. *Neurocomputing*, 600:128133, 2024. doi: 10.1016/J.NEUROCOM.2024.128133. URL <https://doi.org/10.1016/j.neurocom.2024.128133>.

[19] Yalin E. Sagduyu, Tugba Erpek, Sennur Ulukus, and Aylin Yener. Vulnerabilities of deep learning-driven semantic communications to backdoor (trojan) attacks. In *57th Annual Conference on Information Sciences and Systems, CISS 2023, Baltimore, MD, USA, March 22-24, 2023*, pages 1–6. IEEE, 2023. doi: 10.1109/CISS56502.2023.10089692. URL <https://doi.org/10.1109/CISS56502.2023.10089692>.

[20] Xiaodong Xu, Yue Chen, Bishu Wang, Zhiqiang Bian, Shujun Han, Chen Dong, Chen Sun, Wenqi Zhang, Lexi Xu, and Ping Zhang. CSBA: covert semantic backdoor attack against intelligent connected vehicles. *IEEE Trans. Veh. Technol.*, 73(11):17923–17928, 2024. doi: 10.1109/TVT.2024.3427713. URL <https://doi.org/10.1109/TVT.2024.3427713>.

[21] Yinzhi Cao, Alexander Fangxiao Yu, Andrew Aday, Eric Stahl, Jon Merwine, and Junfeng Yang. Efficient repair of polluted machine learning systems via causal unlearning. In *Proceedings of the 2018 on Asia conference on computer and communications security*, pages 735–747, 2018.

[22] Andrea Paudice, Luis Muñoz-González, and Emil C Lupu. Label sanitization against label flipping poisoning attacks. In *ECML PKDD 2018 Workshops: Nemesis 2018, UrbReas 2018, SoGood 2018, IWAISe 2018, and Green Data Mining 2018, Dublin, Ireland, September 10-14, 2018, Proceedings 18*, pages 5–15. Springer, 2019.

[23] Min Du, Ruoxi Jia, and Dawn Song. Robust anomaly detection and backdoor attack detection via differential privacy. *arXiv preprint arXiv:1911.07116*, 2019.

[24] Jonathan Hayase, Weihao Kong, Raghav Somani, and Sewoong Oh. Spectre: Defending against backdoor attacks using robust statistics. In *International Conference on Machine Learning*, pages 4129–4139. PMLR, 2021.

[25] Bryant Chen, Wilka Carvalho, Nathalie Baracaldo, Heiko Ludwig, Benjamin Edwards, Taesung Lee, Ian Molloy, and Biplav Srivastava. Detecting backdoor attacks on deep neural networks by activation clustering. *arXiv preprint arXiv:1811.03728*, 2018.

[26] Dongxian Wu and Yisen Wang. Adversarial neuron pruning purifies backdoored deep models. *Advances in Neural Information Processing Systems*, 34:16913–16925, 2021.

[27] IARPA. Trojai leaderboards, 2020. URL <https://pages.nist.gov/trojai/>. Accessed: 2024-09-12.

[28] Guangyu Shen, Yingqi Liu, Guanhong Tao, Shengwei An, Qiuiling Xu, Siyuan Cheng, Shiqing Ma, and Xiangyu Zhang. Backdoor scanning for deep neural networks through k-arm optimization. In *International Conference on Machine Learning*, pages 9525–9536. PMLR, 2021.

[29] Matt Fredrikson, Somesh Jha, and Thomas Ristenpart. Model inversion attacks that exploit confidence information and basic countermeasures. In Indrajit Ray, Ninghui Li, and Christopher Kruegel, editors, *Proceedings of the 22nd ACM SIGSAC Conference on Computer and Communications Security, Denver, CO, USA, October 12-16, 2015*, pages 1322–1333. ACM, 2015. doi: 10.1145/2810103.2813677. URL <https://doi.org/10.1145/2810103.2813677>.

[30] Bolun Wang, Yuanshun Yao, Shawn Shan, Huiying Li, Bimal Viswanath, Haitao Zheng, and Ben Y. Zhao. Neural cleanse: Identifying and mitigating backdoor attacks in neural networks. In *2019 IEEE Symposium on Security and Privacy (SP)*, pages 707–723, 2019. doi: 10.1109/SP.2019.00031.

[31] Ren Wang, Gaoyuan Zhang, Sijia Liu, Pin-Yu Chen, Jinjun Xiong, and Meng Wang. Practical detection of trojan neural networks: Data-limited and data-free cases. In Andrea Vedaldi, Horst Bischof, Thomas Brox, and Jan-Michael Frahm, editors, *Computer Vision – ECCV 2020*, pages 222–238, Cham, 2020. Springer International Publishing. ISBN 978-3-030-58592-1.

[32] Junfeng Guo, Yiming Li, Xun Chen, Hanqing Guo, Lichao Sun, and Cong Liu. SCALE-UP: an efficient black-box input-level backdoor detection via analyzing scaled prediction consistency. In *The Eleventh International Conference on Learning Representations, ICLR 2023, Kigali, Rwanda, May 1-5, 2023*. OpenReview.net, 2023. URL <https://openreview.net/forum?id=o0LFPcoFKnr>.

[33] Yansong Gao, Chang Xu, Derui Wang, Shiping Chen, Damith Chinthana Ranasinghe, and Surya Nepal. STRIP: a defence against trojan attacks on deep neural networks. In David M. Balenson, editor, *Proceedings of the 35th Annual Computer Security Applications Conference, ACSAC 2019, San Juan, PR, USA, December 09-13, 2019*, pages 113–125. ACM, 2019. doi: 10.1145/3359789.3359790. URL <https://doi.org/10.1145/3359789.3359790>.

[34] S. Kolouri, A. Saha, H. Pirsiavash, and H. Hoffmann. Universal litmus patterns: Revealing backdoor attacks in cnns. In *2020 IEEE/CVF Conference on Computer Vision and Pattern Recognition (CVPR)*, pages 298–307, Los Alamitos, CA, USA, jun 2020. IEEE Computer Society. doi: 10.1109/CVPR42600.2020.00038. URL <https://doi.ieee.org/10.1109/CVPR42600.2020.00038>.

[35] Songzhu Zheng, Yikai Zhang, Hubert Wagner, Mayank Goswami, and Chao Chen. Topological detection of trojaned neural networks. In M. Ranzato, A. Beygelzimer, Y. Dauphin, P.S. Liang, and J. Wortman Vaughan, editors, *Advances in Neural Information Processing Systems*, volume 34, pages 17258–17272. Curran Associates, Inc., 2021.

[36] Yingqi Liu, Guangyu Shen, Guanhong Tao, Zhenting Wang, Shiqing Ma, and Xiangyu Zhang. Complex backdoor detection by symmetric feature differencing. In *2022 IEEE/CVF Conference on Computer Vision and Pattern Recognition (CVPR)*, pages 14983–14993, 2022. doi: 10.1109/CVPR52688.2022.01458.

[37] Bing Sun, Jun Sun, Wayne Koh, and Jie Shi. Neural network semantic backdoor detection and mitigation: A causality-based approach. In Davide Balzarotti and Wenyuan Xu, editors, *33rd USENIX Security Symposium, USENIX Security 2024, Philadelphia, PA, USA, August 14-16, 2024*. USENIX Association, 2024. URL <https://www.usenix.org/conference/usenixsecurity24/presentation/sun-bing>.

[38] Chunlong Xie, Jialing He, Ying Yang, Shangwei Guo, Tianwei Zhang, and Tao Xiang. Semantic and precise trigger inversion: Detecting backdoored language models. *IEEE Trans. Inf. Forensics Secur.*, 20:8096–8108, 2025. doi: 10.1109/TIFS.2025.3594037. URL <https://doi.org/10.1109/TIFS.2025.3594037>.

[39] Yuan Zhou, Rose Qingyang Hu, and Yi Qian. Backdoor attacks and defenses on semantic-symbol reconstruction in semantic communications. In *IEEE International Conference on Communications, ICC 2024, Denver, CO, USA, June 9–13, 2024*, pages 734–739. IEEE, 2024. doi: 10.1109/ICC51166.2024.10622193. URL <https://doi.org/10.1109/ICC51166.2024.10622193>.

[40] Pratyush Maini, Mohammad Yaghini, and Nicolas Papernot. Dataset inference: Ownership resolution in machine learning. In *Proceedings of the 2021 International Conference on Learning Representations (ICLR 2021)*, 2021.

[41] Yiming Li, Linghui Zhu, Xiaojun Jia, Yong Jiang, Shu-Tao Xia, and Xiaochun Cao. Defending against model stealing via verifying embedded external features. In *AAAI*, 2022.

[42] Hengrui Jia, Christopher A Choquette-Choo, Varun Chandrasekaran, and Nicolas Papernot. Entangled watermarks as a defense against model extraction. In *30th USENIX security symposium (USENIX Security 21)*, pages 1937–1954, 2021.

[43] Sebastian Szyller, Buse Gul Atli, Samuel Marchal, and N Asokan. Dawn: Dynamic adversarial watermarking of neural networks. In *Proceedings of the 29th ACM International Conference on Multimedia*, pages 4417–4425, 2021.

[44] Xiaoyu Cao, Jinyuan Jia, and Neil Zhenqiang Gong. IPGuard: Protecting intellectual property of deep neural networks via fingerprinting the classification boundary. In *Proceedings of the 2021 ACM Asia Conference on Computer and Communications Security*, pages 14–25, 2021.

[45] Yuanchun Li, Ziqi Zhang, Bingyan Liu, Ziyue Yang, and Yunxin Liu. ModelDiff: Testing-based dnn similarity comparison for model reuse detection. In *Proceedings of the 30th ACM SIGSOFT International Symposium on Software Testing and Analysis, ISSTA 2021*, page 139–151, New York, NY, USA, 2021. Association for Computing Machinery. ISBN 9781450384599. doi: 10.1145/3460319.3464816. URL <https://doi.org/10.1145/3460319.3464816>.

[46] Aleksander Madry, Aleksandar Makelov, Ludwig Schmidt, Dimitris Tsipras, and Adrian Vladu. Towards deep learning models resistant to adversarial attacks. In *International Conference on Learning Representations*, 2018. URL <https://openreview.net/forum?id=rJzIBfZAb>.

[47] Ian J. Goodfellow, Jonathon Shlens, and Christian Szegedy. Explaining and harnessing adversarial examples. In *3rd International Conference on Learning Representations (ICLR)*, 2015. URL <https://arxiv.org/abs/1412.6572>.

[48] Alex Schlägl, Nora Hofer, and Rainer Böhme. Causes and effects of unanticipated numerical deviations in neural network inference frameworks. In *Proc. NeurIPS*, 2023. URL https://proceedings.neurips.cc/paper_files/paper/2023/hash/af076c3bdf935b81d808e37c5ede463-Abstract-Conference.html.

[49] William J Youden. Index for rating diagnostic tests. *Cancer*, 3(1):32–35, 1950.

[50] David M. W. Powers. Evaluation: from precision, recall and F-measure to ROC, informedness, markedness and correlation. *CoRR*, abs/2010.16061, 2020. URL <https://arxiv.org/abs/2010.16061>.

[51] Dmitry Ulyanov, Andrea Vedaldi, and Victor Lempitsky. Deep image prior. In *Proceedings of the IEEE conference on computer vision and pattern recognition*, pages 9446–9454, 2018.

[52] Jimmy Ba and Diederik Kingma. Adam: A method for stochastic optimization. In *3rd International Conference on Learning Representations (ICLR)*, 2015. URL <http://arxiv.org/abs/1412.6980>.

[53] Alex Krizhevsky. Learning multiple layers of features from tiny images. Technical report, University of Toronto, 2009. URL <https://www.cs.toronto.edu/~kriz/learning-features-2009-TR.pdf>.

[54] Jeremy Howard. Imagenette: A smaller subset of 10 easily classified classes from imagenet, March 2019. URL <https://github.com/fastai/imagenette>.

[55] Jia Deng, Wei Dong, Richard Socher, Li-Jia Li, Kai Li, and Li Fei-Fei. Imagenet: A large-scale hierarchical image database. In *2009 IEEE Computer Society Conference on Computer Vision and Pattern Recognition (CVPR 2009), 20–25 June 2009, Miami, Florida, USA*, pages 248–255. IEEE Computer Society, 2009. doi: 10.1109/CVPR.2009.5206848. URL <https://doi.org/10.1109/CVPR.2009.5206848>.

[56] Kaiming He, Xiangyu Zhang, Shaoqing Ren, and Jian Sun. Deep residual learning for image recognition. In *The IEEE Conference on Computer Vision and Pattern Recognition (CVPR)*, June 2016. URL https://www.cv-foundation.org/openaccess/content_cvpr_2016/papers/He_Deep_Residual_Learning_CVPR_2016_paper.pdf.

[57] Sven Gowal, Sylvestre-Alvise Rebuffi, Olivia Wiles, Florian Stimberg, Dan Andrei Calian, and Timothy A Mann. Improving robustness using generated data. In M. Ranzato, A. Beygelzimer, Y. Dauphin, P.S. Liang, and J. Wortman Vaughan, editors, *Advances in Neural Information Processing Systems*, volume 34, pages 4218–4233. Curran Associates, Inc., 2021.

[58] Jonathan Ho, Ajay Jain, and Pieter Abbeel. Denoising diffusion probabilistic models. In H. Larochelle, M. Ranzato, R. Hadsell, M.F. Balcan, and H. Lin, editors, *Advances in Neural Information Processing Systems*, volume 33, pages 6840–6851. Curran Associates, Inc., 2020.

[59] Francesco Croce and Matthias Hein. Reliable evaluation of adversarial robustness with an ensemble of diverse parameter-free attacks. In *Proceedings of the 37th International Conference on Machine Learning, ICML 2020, 13-18 July 2020, Virtual Event*, volume 119 of *Proceedings of Machine Learning Research*, pages 2206–2216. PMLR, 2020. URL <http://proceedings.mlr.press/v119/croce20b.html>.

[60] Sergey Zagoruyko and Nikos Komodakis. Wide residual networks. In Richard C. Wilson, Edwin R. Hancock, and William A. P. Smith, editors, *Proceedings of the British Machine Vision Conference 2016, BMVC 2016, York, UK, September 19-22, 2016*. BMVA Press, 2016. URL <http://www.bmva.org/bmvc/2016/papers/paper087/index.html>.

[61] Sanghyun Woo, Shoubhik Debnath, Ronghang Hu, Xinlei Chen, Zhuang Liu, In So Kweon, and Saining Xie. Convnext V2: co-designing and scaling convnets with masked autoencoders. In *IEEE/CVF Conference on Computer Vision and Pattern Recognition, CVPR 2023, Vancouver, BC, Canada, June 17-24, 2023*, pages 16133–16142. IEEE, 2023. doi: 10.1109/CVPR52729.2023.01548. URL <https://doi.org/10.1109/CVPR52729.2023.01548>.

[62] Seunghoon Lee, Seunghyun Lee, and Byung Cheol Song. Improving vision transformers to learn small-size dataset from scratch. *IEEE Access*, 10:123212–123224, 2022. doi: 10.1109/ACCESS.2022.3224044.

[63] Ilya Loshchilov and Frank Hutter. Decoupled weight decay regularization. In *7th International Conference on Learning Representations, ICLR 2019, New Orleans, LA, USA, May 6-9, 2019*. OpenReview.net, 2019. URL <https://openreview.net/forum?id=Bkg6RiCqY7>.

[64] Qiong Cao, Li Shen, Weidi Xie, Omkar M Parkhi, and Andrew Zisserman. Vggface2: A dataset for recognising faces across pose and age. In *2018 13th IEEE international conference on automatic face & gesture recognition (FG 2018)*, pages 67–74. IEEE, 2018.

[65] Geoffrey Hinton, Oriol Vinyals, and Jeffrey Dean. Distilling the knowledge in a neural network. In *NIPS Deep Learning and Representation Learning Workshop*, 2015.

[66] Yige Li, Xixiang Lyu, Nodens Koren, Lingjuan Lyu, Bo Li, and Xingjun Ma. Neural attention distillation: Erasing backdoor triggers from deep neural networks. In *9th International Conference on Learning Representations, ICLR 2021, Virtual Event, Austria, May 3-7, 2021*. OpenReview.net, 2021. URL <https://openreview.net/forum?id=910K40M-oXE>.